Chapter 3
Methodology

Sven Teske, Thomas Pregger, Sonja Simon, Tobias Naegler, Johannes Pagenkopf, Bent van den Adel, Malte Meinshausen, Kate Dooley, C. Briggs, E. Dominish, D. Giurco, Nick Florin, Tom Morris, and Kriti Nagrath

Abstract A detailed overview of the methodologies used to develop the 2.0 °C and 1.5 °C scenario presented in this book. Starting with the overall modelling approach, the interaction of seven different models is explained which are used to calculate and developed detailed scenarios for greenhouse gas emission and energy pathways to stay within a 2.0 °C and 1.5 °C global warming limit. The following models are presented:

- For the non-energy GHG emission pathways, the *Generalized Equal Quantile Walk (GQW)* method, the land-based sequestration design method and the Carbon cycle and climate (MAGICC) model.
- For the energy pathways, a renewable energy resources assessment for space constrained environments ([R]E-SPACE, the transport scenario model (TRAEM), the Energy System Model (EM) and the power system model [R]E 24/7.

The methodologies of an employment analysis model, and a metal resource assessment tool are outlined. These models have been used to examine the analysis of the energy scenario results.

S. Teske (✉) · C. Briggs · E. Dominish · D. Giurco · N. Florin · T. Morris · K. Nagrath
Institute for Sustainable Futures, University of Technology Sydney, Sydney, NSW, Australia
e-mail: sven.teske@uts.edu.au; chris.briggs@uts.edu.au; elsa.dominish@uts.edu.au; damien.giurco@uts.edu.au; nick.florin@uts.edu.au; tom.morris@uts.edu.au; kriti.nagrath@uts.edu.au

T. Pregger · S. Simon · T. Naegler
Department of Energy Systems Analysis, German Aerospace Center (DLR), Institute for Engineering Thermodynamics (TT), Pfaffenwaldring, Germany
e-mail: thomas.pregger@dlr.de; sonja.simon@dlr.de; tobias.naegler@dlr.de

J. Pagenkopf · B. van den Adel
Department of Vehicle Systems and Technology Assessment, German Aerospace Center (DLR), Institute of Vehicle Concepts (FK), Pfaffenwaldring, Germany
e-mail: johannes.pagenkopf@dlr.de; Bent.vandenAdel@dlr.de

M. Meinshausen · K. Dooley
Australian-German Climate and Energy College, University of Melbourne, Parkville, Victoria, Australia
e-mail: malte.meinshausen@unimelb.edu.au; kate.dooley@unimelb.edu.au

S. Teske (ed.), *Achieving the Paris Climate Agreement Goals*,
https://doi.org/10.1007/978-3-030-05843-2_3

Achieving the goals of the Paris Climate Agreement (UNFCCC 2015) will require the total decarbonisation of the energy system by 2050, with a global emissions peak no later than 2020 (Hare and Roming 2016) and a drastic reduction in non-energy-related greenhouse gases (GHGs), including land-use-related emissions (Rogelj and den Elzen 2016). Over the past decades, numerous computer models have been developed to analyse different emissions pathways and to investigate the effects of changes in policy and technology and adjustments in global and regional economies. A wide range of climate models is used to calculate non-energy-related GHG emissions pathways and their impacts on the global climate. The Intergovernmental Panel on Climate Change (IPCC) states that "Climate models have continued to be developed and improved since the AR4 [published in 2007-author], and many models have been extended into Earth System models by including the representation of biogeochemical cycles important to climate change" (Flato and Marotzke 2013). Whereas climate models analyse the effects of a variety of GHG emissions, energy scenarios only cover energy-related CO_2. Their purpose is to investigate future energy systems to identify feasible technological and/or economic pathways. Like climate models, energy models are diverse and vary significantly in their methodologies. The IPCC's Special Report on Renewable Energy Sources and Climate Change Mitigation states that there is "enormous variation in the detail and structure of the models used to construct the scenarios" (Fischedick and Schaeffer 2011). Energy scenarios with high penetrations of variable renewable power generation—solar photovoltaic (PV) and wind power—require a higher degree of time resolution to assess the security of 24/7 electricity supplies than those with mainly dispatchable power generation.

Modelling the energy system involves a variety of methodological requirements, which pose specific challenges when addressed on the global level: the quantitative projection of developments in (future) technologies and potential markets; a consistent database of renewable energy potentials and their temporal and spatial distributions; reliable data on the current situations in all regions; an assessment of energy flows and emissions across all energy subsectors, such as industry, transport, residential, etc.; and a comprehensive assessment of all CO_2 emissions, in order to assess the impact of the energy system on climate change. Finally, analysing and assessing the energy transition require a long-term perspective on future developments.

Changes to energy markets require long-term decisions to be made because infrastructural changes are potentially required, and are therefore independent of short-term market developments. The power market cannot function optimally without long-term infrastructure planning. Grid modifications and the roll-out of smart metering infrastructure, for example, require several years to implement. These technologies form the basis of the energy market and allow energy trading. Therefore, the time required for infrastructure planning and other substantial transformation processes must be considered in the scenario-building approach.

Although numerous energy scenarios that provide 100% renewable energy at the community, state, and national levels have been published in the past decade (Elliston and MacGill 2014; Teske and Dominish 2016; Klaus et al. 2010; Teske and Brown 2012), only a handful of analyses have been performed on a global level. The main research projects on 100% renewable energy supplies published between 2015 and 2018 were:

– A Road Map to 100 Percent Renewable Energy in 139 Countries by 2050, Mark Jacobson, Charles Q. Choi, Stanford Engineering, Stanford University, USA, 2017 (Jacobson and Choi 2017);
– Internet of Energy, A 100% Renewable Electricity System, Christian Breyer, Neo Carbon Energy, Lappeenranta University of Technology, Finland, 2016 (Breyer 2016; Breyer and Bogdanov 2018);
– Energy [R]evolution—A sustainable World Energy Outlook 2015, Greenpeace International with the German Aerospace Centre (DLR), Institute of Engineering Thermodynamics, System Analysis and Technology Assessment, Stuttgart, Germany (Teske and Pregger 2015).

All the studies listed above share the same modelling horizon until 2050 and focus clearly on the fast and massive deployment of renewable energy resources (RES). Options with large uncertainties in terms of techno-economic, societal, and environmental risks, such as large hydro power, nuclear power, or unsustainable biomass use, carbon capture and storage (CCS), and geoengineering are excluded. However, each of these studies has a specific strength. On the one hand, the analyses from Stanford University and the University of Technology Lappeenranta include an hourly simulation of power demand and supply, in addition to the pathway modelling. On the other hand, the Energy [R]evolution study covers the complete energy sector, with detailed insights into the heat and transport sectors. However, all these studies cover only CO_2 emissions from the energy system, without further investigation of other GHG sources.

Therefore, our project combines these strengths into a single approach by combining a set of models. The approach is based on the scenario modelling used for the Energy [R]evolution scenario series developed by the authors between 2004 and 2015. It models scenarios of comprehensive pathways for power, heat, and fuel supply in 5-year steps, and includes specific insights from a transport model. The scenario building is also complemented by a simulation with hourly resolution to calculate the electricity storage demand and to increase the spatial resolution from 10 to 72 regions. Another significant improvement over existing studies is its combination with a climate model. The interaction between non-energy GHG pathways and a high-resolution integrated energy assessment model (IAM) provides additional information on how to achieve the goals of the Paris Agreement.

3.1 100% Renewable Energy—Modelling Approach

The complete decarbonisation of the global energy supply requires entirely new technical, economic, and policy frameworks for the electricity, heating, and cooling sectors, and the transport system. Such new framework conditions and the political and regulative interventions necessary for their implementation are widely discussed in the literature. However, assessing their feasibility and effectiveness requires an in-depth analysis of specific regional and national conditions and mechanisms. Therefore, societal frameworks, measures, and policy interventions are not explicitly discussed in this scenario analysis, but they are implicit elements in the definition of the narratives and assumptions as core step of scenario development (see Chap. 5).

Modelling Approach

To develop a global plan, the authors combined various established computer models:

- Global GHG Model: The non-energy GHG emissions scenarios are calculated with the following models:
  - Generalized Equal Quantile Walk (GQW): This statistical method is used to complement the CO_2 pathways with the non-CO_2 regional emissions for the relevant GHGs and aerosols, based on a statistical analysis of the large number (~700) of multi-gas emission pathways underlying the recent IPCC Fifth Assessment Report and the recently published IPCC Special Report on 1.5 °C. The GQW method calculates the median non-CO_2 gas emission levels every 5 years, conditional on the energy-related CO_2 emission level percentile of the 'source' pathway. This method is further developed in this project—building on an earlier 'Equal Quantile Walk' method—and is now better able to capture the emission dynamics of low-mitigation pathways.
  - Land-based sequestration design: A Monte Carlo analysis across temperate, boreal, subtropical, and tropical regions has been performed based on various literature-based estimates of sequestration rates, sequestration periods, and the areas available for a number of sequestration options. This approach can be seen as a quantified literature synthesis of the potential for land-based CO_2 sequestration, which is not reliant on bioenergy with sequestration and storage (BECCS)
  - Carbon cycle and climate modelling (MAGICC): This study used the MAGICC climate model, which also underlies the classification of both the IPCC Fifth Assessment Report and the IPCC Special Report on 1.5 °C in terms of the ability of various scenarios to limit the temperature increase to below 2.0 °C or 1.5 °C. MAGICC is constantly evolving, but its core goes back to the 1980s, and it represents one of the most established reduced-complexity climate models in the international community.
- Renewable Resource Assessment [R]E-SPACE: This is based on a Geographic Information Systems (GIS) approach and provides maps of the solar and wind potentials in space-constrained environments. GIS attempts to emulate processes in the real world, at a single point in time or over an extended period (Goodchild 2005). The primary purpose of GIS mapping is to ascertain whether renewable energy resources (primarily solar and wind) are sufficiently available in each region. It also provides an overview of the existing electricity infrastructures for fossil fuel and renewable sources.
- Transport model (TRAEM): The transport scenario model allows the representation of long-term transport developments in a consistent and transparent way. The model disaggregates transport into a set of different modes and calculates the final energy demand by multiplying the specific transport demand of each transport mode with the powertrain-specific energy demands, using passenger–km and tonne–km activity-based bottom-up approaches. The model applied is an accounting system, without system or ownership cost-optimization.
- Energy system model (EM): The scenario model is a mathematical accounting system for the energy sector that applies different methodologies. It aims to

model the development of energy demand and supply according to the energy potentials, future costs, emissions, specific fuel consumptions, and physical flows between processes. The data available and the objectives of the analysis significantly influence the model architecture and approach. It is very important to differentiate between an energy model and a scenario. An energy model is the technical basis for a scenario. Scenarios are the results of the energy model, which have been calculated with different input data and assumptions. The energy model is used in this study to develop long-term scenarios for the energy systems across all sectors (power, heat, transport, and industry) without the application of cost-optimization based on uncertain cost assumptions. However, an ex-post analysis of costs and investments shows the main economic effects of the pathways.

- Power system model [R]E 24/7: This simulates the electricity system on an hourly basis and at geographic resolution to assess the requirements for infrastructure, such as grid connections, between different regions and electricity storages, depending on the demand profiles and power-generation characteristics (Teske 2015). High-penetration or renewable-energy-only scenarios will contain significant proportions of variable solar photovoltaic (PV) and wind power because they are inexpensive. Therefore, a power system model is required to assess the demand and supply patterns, the efficiency of power generation, and the resulting infrastructural needs. On the generation side, meteorological data, typically in 1 h steps, are required and historical solar and wind data are used to calculate the possible renewable power generation. On the demand side, either historical demand curves are used, or—if unavailable—demand curves are calculated based on assumptions of consumer behaviour, the electrical equipment and common electrical appliances.

Figure 3.1 provides an overview of the interactions between the energy- and GIS-based models. The climate model is not directly connected but provided the probabilistic temperatures for the 2.0 °C and 1.5 °C Scenarios. The land-use and non-CO_2 emissions modules provide information on additional gases based on the energy-related CO_2 emissions (output of the energy model). Besides the climate and energy models, the effects on employment and the requirements for selected metal resources have been calculated (see Sects. 3.6 and 3.7).

3.2 Global Mapping—Renewable Energy Potential in Space-Constrained Environments: [R]E-SPACE

The primary purpose of GIS mapping is to ascertain the renewable energy resources (primarily solar and wind) available in each region. It also provides an overview of the existing electricity infrastructures for fossil fuel and renewable sources.

In this project, mapping was undertaken with the computer software QGIS. QGIS is a free, cross-platform, open-source desktop GIS application that supports the viewing, editing, and analysis of geo-spatial data. It analyses and edits spatial information and composes and exports graphical maps, and was used to allocate solar

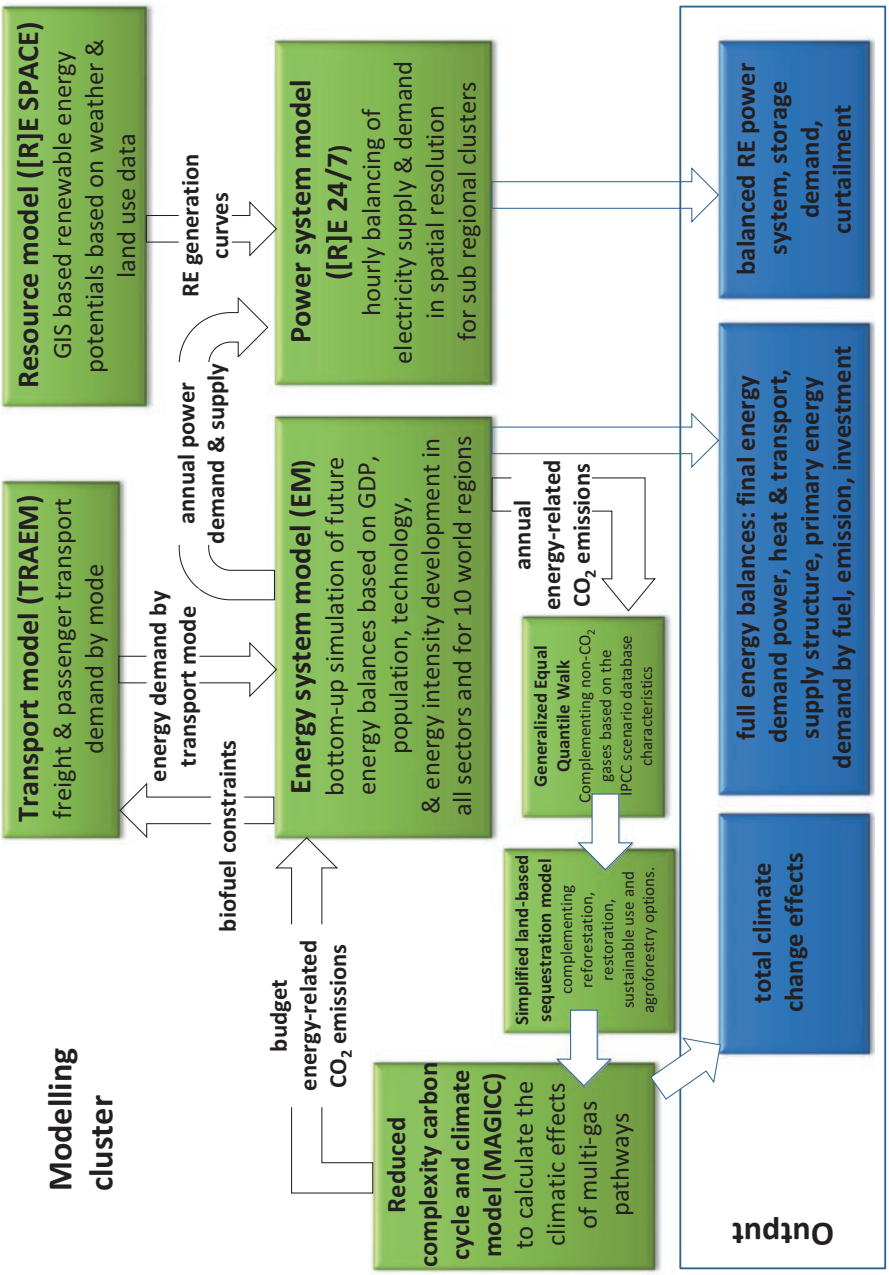

Fig. 3.1 Interaction of models in this study

Table 3.1 Overview of regions and sub-regions used in the analysis

Regions	Cluster/Sub-regions	Regions	Cluster / Sub-regions
North America	USA-Alaska West Canada East Canada North-West USA North-East USA South-West USA South East USA Mexico Mexico	Eurasia	Central Asia Eastern Europe East Caspian West Caspian Kazakhstan Mongolia Russia
Latin America	Argentina Brazil Caribbean Central America Central—South America Chile North Latin America Uruguay	Non-OECD Asia	Asia West: Pakistan, Afghanistan, Nepal, Bhutan Sri Lanka Asia Central North: Viet Nam, Laos and Cambodia Asia North West: Bangladesh, Myanmar, Thailand Asia South-West: Malaysia, Brunei Pacific Island States Indonesia Philippines
Europe	Balkans & Greece Baltic Central Europe Nordic Iberian Peninsula Turkey UK & Ireland	India	East India North India Northeast India South India including Islands West India
Africa	Central Africa East Africa North Africa South Africa Southern Africa West Africa	China	Central China East China North China Northeast China Northwest China South China Taiwan Tibet
Middle East	East ME North ME Iran Iraq Israel Saud Arabia UAE	OECD Pacific	South Korea North Japan South Japan North New Zealand South New Zealand Australia—NEM Australia—SWIS

and wind resources and for demand projection for each region analysed. Open-source data and maps from various sources were used to visualize each country and its regions and districts. The regions and districts are divided into clusters. The regions are divided along geographic boundaries, using the IEA regions as a guide. Some of the larger countries, such as China and India, have been extracted to create individual scenarios. The clusters are also divided on geographic and political bases. A list of regions and their respective clusters is given in Table 3.1.

Wind speed data at different levels, in metres per second (m/s), were obtained from Vaisala 2017. For this analysis, wind speed at a height of 80 m was used to determine the electricity-generation potential. Wind speeds are categorized and mapped within the range of 5–12 m/s to gain an understanding of the potential generation across the regions. Speeds under 5 m/s are ignored when plotting optimal sites. Land-cover types were constrained to bare soil and grasslands. The model only accounts for the onshore wind-generation potential.

Land-cover data were obtained from the Global Land Cover 2000 project (Global Land Cover 2015), hosted by the European Commission's Joint Research Centre. The classification was based on the FAO Land Cover Classification System.

Similarly, solar resource data were obtained from the Global Solar Atlas (Global Solar Atlas 2016), owned by the World Bank Group and provided by SolarGis. Data categorized by direct normal irradiation were mapped to estimate the potential PVs in the different regions. To avoid conflict with competing uses of land, only the land-cover types 'bare soil' and 'grasslands' were included in the analysis.

The area of land available for potential solar and wind power generation was calculated at the cluster level using the Geometry tool in the QGIS-processing toolbox. Intersects (overlapping areas between different layers) were created between the transmission-level layers and the solar/wind utility vector layers to break down the total land area available into clusters. A correction was put in place manually for sites that intersected the cluster boundaries and were part of two clusters.

For some maps (India, China, the Middle East, and OECD Pacific) with large data files, the analysis was performed using raster files for land use and renewable potentials. The raster tools 'clipper' (used to cut a raster file to the size of the cluster) and 'merge' (used to extract common areas between two layers) were used. This input was fed into the calculations for the [R]E 24/7 Model.

The regional maps illustrate the different clusters that were identified for scenario modelling. The existing infrastructure maps highlight the power plants and transmission networks in the regions. The wind and solar potential maps indicate the land available for new power generation given the current land-use patterns. These maps show utility-scale installations. There are much larger expanses of land available for small-scale distributed energy generation.

The following types of maps were created for 10 world regions:

Regional breakdown into a maximum of eight clusters:

The example given in Fig. 3.2 shows OECD North America—one of the 10 world regions—broken down into eight sub-regions (clusters). The [R]E 24/7 power system analysis (see Sect. 3.5) calculates an electricity demand and supply scenario for each of those eight clusters. The clusters can exchange electricity with each other (see Sect. 3.8).

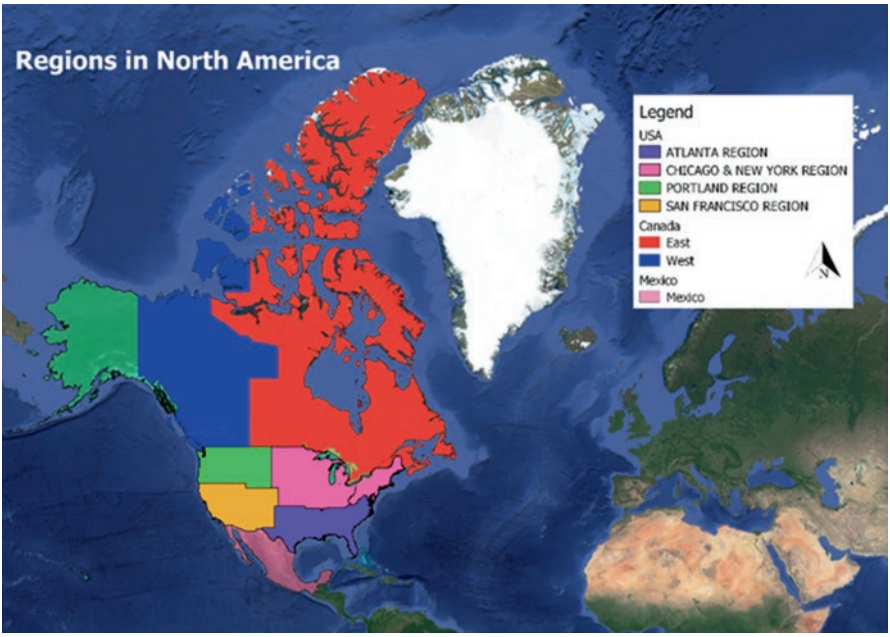

Fig. 3.2 OECD North America broken down into eight sub-regions

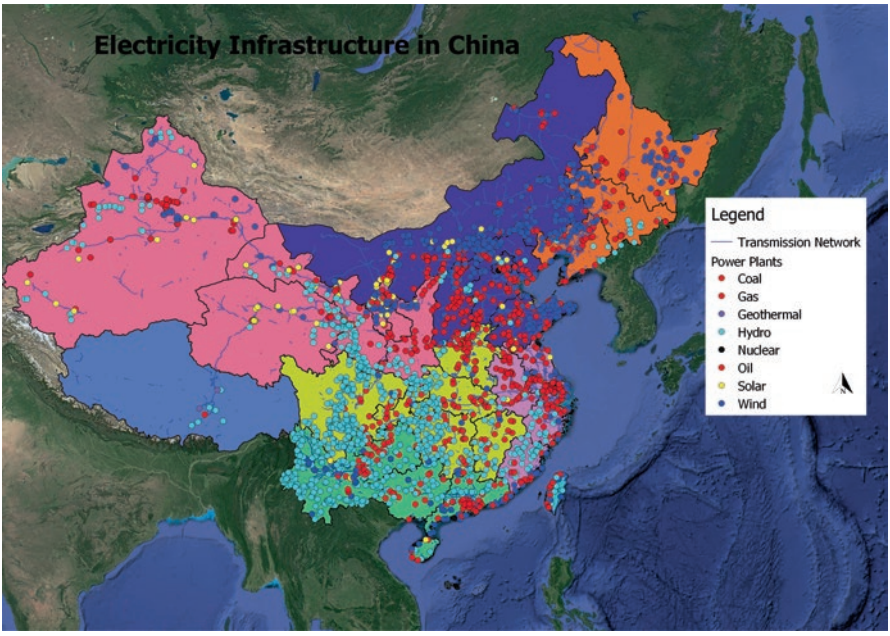

Fig. 3.3 Current electricity infrastructure in China

Current electricity infrastructure

The example given in Fig. 3.3 shows the current electricity infrastructure—power plants generating > 1 MW—and high-voltage transmission lines in China. For the development of future electricity scenarios, it is important to know whether the generation capacity for dispatch and the transmission capacity to transport electricity from utility-scale wind and/or solar power plants to demand centres are available.

Potential sites for onshore wind power

Figure 3.4 gives an overview of the potential onshore wind-power-generation sites in Africa. Only the blue areas are available for new wind development, whereas the remaining regions are used for nature conservation, agriculture, settlement, or other forms of land use that do not allow the installation of wind farms. The darker the blue area, the better the wind potential.

Potential sites for utility-scale solar power plants

Figure 3.5 shows the suitable sites for utility-scale solar power sites in Central and South America. The scale from yellow to orange to red indicates increasing available solar radiation. Red areas—in this example, the Atacama Desert in Chile—indicate the best solar resources and are suitable for both solar PV power plants and concentrated solar power plants.

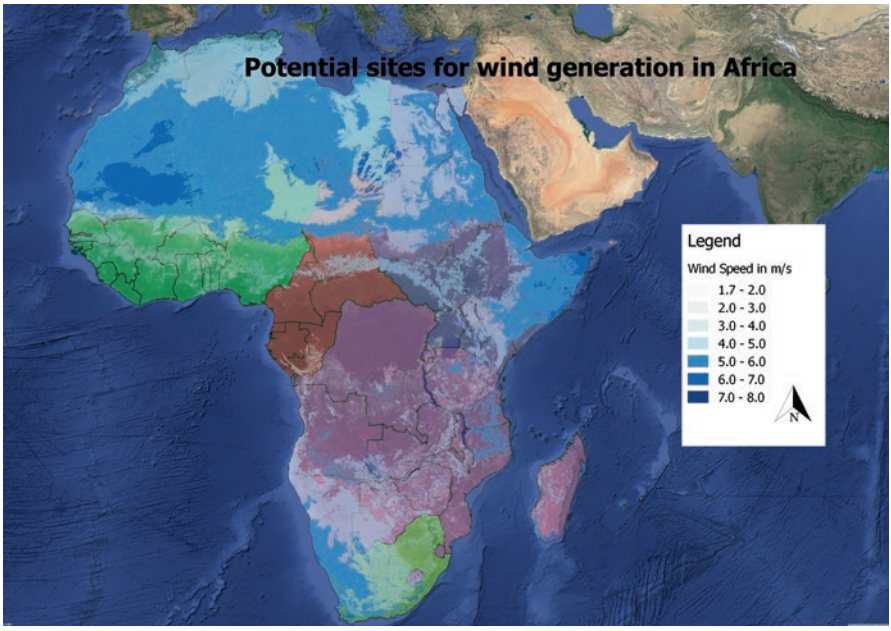

Fig. 3.4 Potential sites for onshore wind generation in Africa

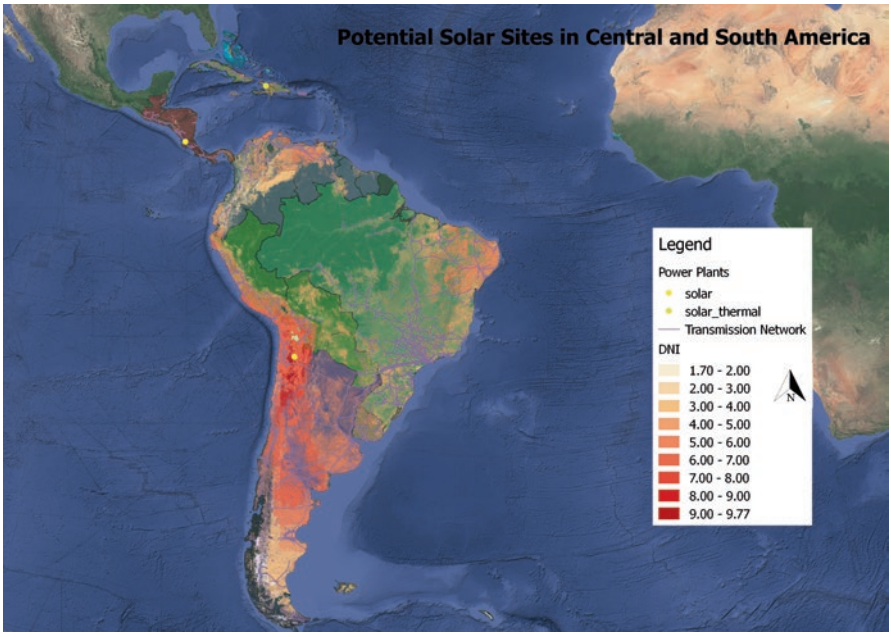

Fig. 3.5 Existing and potential solar power sites in Central and South America

3.3 Transport Energy Model-TRAEM

3.3.1 Transport Model Structure

The transport scenario model TRAEM (TRAnsport Energy Model) allows the modelling of long-term transport developments for the 10 world regions. It is divided into several sub-models according to the transport modes, which are discussed below. All 10 world regions are aggregated in the world model using a passenger–km (pkm) and tonne–km (tkm) activity-based bottom-up approach. The model calculates the final energy demand by multiplying the specific transport demand of each transport mode with the powertrain-specific energy demands. This gives the annual energy demand for electricity, fossil fuels (diesel, petrol), natural gas, bio-based fuels, synthetically produced fuels (also called 'synfuels'), and hydrogen for each of the 10 world regions. The calculation is performed in 5-year steps, from 2015 to 2050.

For all scenarios (5.0 °C, 2.0 °C, and 1.5 °C), the 2015 energy demand by region was adjusted to the IEA World Energy Balances 2017 and is therefore identical in all scenarios. The projected total energy demands for the reference scenario (5.0 °C) from 2020 until 2040 follow the IEA World Energy Outlook 2017 Current Policies Scenario (IEA 2017b). The total energy demands by region for the years 2045 and 2050 were extrapolated linearly based on the 2035–2040 change rates. The 2.0 °C

Scenario was adjusted from 2020 onwards to 2050 in line with the carbon budget of the 2.0 °C pathway and the 1.5 °C pathway.

In the transport model, the CO_2 emissions from biofuels are given a GHG emission factor of zero, because the downstream emissions level out with the upstream emissions. The CO_2 emissions from synthetic fuels are also given a value of zero, because the CO_2 used for producing the fuels upstream level out the downstream emissions. The upstream emissions from electricity and hydrogen production and all other fuels are factored into the energy system model described in Section 5 with which the transport model has a data interface. The model distinguishes between road, rail, aviation, and maritime passenger and freight transport modes.

Road passenger transport modes include:

- Light duty vehicles (cars): automobiles, vans and sports utility vehicles with up to eight seats for private transport, which are further distinguished into small, medium and large cars;
- 2- and 3-wheel vehicles: includes rollers, motorbikes, and rickshaws;
- Busses: urban, suburban, and long-distance buses and minibuses serving public and private-company transport services.

Rail passenger:

- Urban metro/light rail vehicles;
- Regional/intercity trains;
- High-speed trains.

Aviation (passenger):

- Small and medium aircrafts for domestic flights;
- Medium and large aircrafts for international flights, distinguishing narrow-body, wide-body, and regional jets.

Road freight:

- Light-duty trucks (< 3.5 t gross vehicle weight [GVW]);
- Medium-duty trucks (3.5–15 t GVW);
- Heavy-duty trucks (> 15 t GVW).

Rail freight:

- Ordinary freight, intermodal, and low-density high-value freight trains are distinguished.

Navigation (freight):

- Inland navigation;
- Coastal ships for domestic navigation and maritime shipping are distinguished in the model.

We assume that energy efficiency improves over time. The changes in the powertrain shares over time are mainly driven by fleet electrification. Energy intensities

per pkm and per tkm are region-dependent, based on the occupancy rates of the passenger transport modes and the loading factors for freight vehicles. The energy demands of all transport modes (passenger and freight) are summed to the total energy demand by region.

Backcasting transport scenarios are modelled iteratively by fitting the drivetrain shares, transport performance (pkm or tkm), and modal shares until the specific downstream CO_2 budgets of the world regions are met. The emission reductions are based on a combination of technical, operational, and behavioural measures during modelling—such as powertrain electrification, the use of biomass-based and synthetically produced fuels, efficiency increases within transport modes, and modal shifts towards more-efficient modes.

The replacement of internal combustion engines by electric powertrains is prioritized in our modelling. However, the rapid electrification of fleets is quantity-restricted over the immediately subsequent years until the capacities for battery production, battery recharging, hydrogen production, and refuelling stations have ramped up ubiquitously. Therefore, a shift towards more energy-efficient and electrified passenger and freight transport modes, such as railways, is required and is therefore one measure implemented in the model. Such modal shifts are especially required in the OECD countries, to reduce carbon emissions while maintaining transport performance at the current levels. Supply constraints on biomass and especially synfuel production will also limit rapid decarbonisation right from the start, and motivate modal shifts and general restrictions to overall transport activities by carbon-intensive transport modes. The 1.5 °C Scenario requires electrification, modal shifts, and alternative fuel uptake to start earlier than the 2.0 °C Scenario and particularly the 5.0 °C Scenario, and their more rapid implementation. However, because electrification will remain quantity-restricted until the 2020s in any case, widespread modal shifts and changes in mobility behaviour are modelled more stringently within the 1.5 °C Scenario. The detailed modelling results are discussed in Chap. 6.

3.3.2 Transport Data

We have derived historical and current data on transport activities (pkm, tkm) and total energy consumption levels according to transport mode from statistical agencies, governmental and intergovernmental organizations, etc., including:

- IEA Mobility Model;
- OECD statistics;
- World Bank Open Data;
- National and supranational statistical bodies;
- UIC IEA Railway Handbook;
- UIC Railway Synopsis;
- Railway operators data;

– HBEFA (Handbuch Emissionsfaktoren);
– EIA Open Data.

However, statistical data are often unavailable or lack consistency with other derived data (for example, on vehicle stock or occupancy rates in certain world regions). In these cases, we applied best guesses based on the scientific and grey literature. Data for energy intensity per transport mode were derived from the German Aerospace Centre (DLR) vehicle databases and the state-of-the-art literature.

3.3.3 Transport Model Output

Based on the TRAEM model, energy consumption and CO_2 emissions can be calculated for each transport sub-category.

The final energy demand (ED) of the passenger and freight transport modes is calculated for every world region and all powertrains in 5-year steps from 2015 to 2050 in the following way:

$$TTED(t) = \sum_{wr=1}^{WR} \sum_{m=1}^{M} \sum_{i=1}^{I} TPP_{m,i}^{wr}(t) \times SECP_{m,i}^{wr}(t) + TPF_{m,i}^{wr}(t) \times SECF_{m,i}^{wr}(t)$$

with:

– $SECF_{m,i}^{wr}(t)$: specific freight mode energy consumption of powertrain *i* and mode *m* in world region *wr* at time step *t* [MJ/tkm]
– $SECP_{m,i}^{wr}(t)$: specific passenger mode energy consumption of powertrain *i* and mode *m* in world region *wr* at time step *t* [MJ/pkm]
– $TPF_{m,i}^{wr}(t)$: freight transport performance of powertrain *i* and mode *m* in world region *wr* at time step *t* [tkm/a]
– $TPP_{m,i}^{wr}(t)$: passenger transport performance of powertrain *i* and mode *m* in world region *wr* at time step *t* [pkm/a]
– TTED(t): total transport (final) energy demand at time step *t* [PJ/year]

The estimated plug-in hybrid electric vehicles, battery electric vehicles, and fuel-cell-electric vehicles stocks are considered mode by mode, using their respective battery capacities, vehicle-specific life expectancies, total battery capacity by mode, world region, and year, to estimate the total transport battery demand (Chap. 11).

3.4 Energy System Model (EM)

The focus of this study is the development of normative, long-term scenarios. The scenarios are target-oriented. Starting from the identified desirable future in 2050, they use a backcasting process to deliver potential transformation pathways for the energy system. Technical bottom-up scenarios are developed to meet the climate targets in terms of cumulative CO_2 emissions and are then compared with a reference case. The scenarios are based on detailed input data sets that consider defined targets, renewable and fossil fuel energy potentials, and specific parameters for power, heat, and fuel generation in the energy systems. The scenarios are represented in the Energy System model (EM) developed by the DLR, which is implemented in the energy simulation platform Mesap/PlaNet (Seven2one 2012; Schlenzig 1998). Mesap/PlaNet is an accounting framework that allows the calculation of detailed and complete energy system balances, from demand to energy supply, in 5-year steps up to 2050. The model consists of two independent modules:

- a flow calculation module, which balances energy supply and demand annually, and
- a cost calculation module for the calculation of the corresponding investment, generation, and fuel costs.

The strength of the model framework is in its flexible and transparent modelling of different normative paths. The approach requires exogenously defined expansion rates and market shares. It explicitly renounces economic optimization because of the uncertainty of long-term cost assumptions. Therefore, scenario development using this modelling approach is mainly based on background knowledge and derived narratives, and the experience and knowledge of the scenario developer is essential to the success of the scenario-building process. The model acts as a framework for integrating a wide variety of aspects of the transformation of energy systems, and therefore differs fundamentally from optimization models. The standardized cost calculation for the power sector is used for the ex-post evaluation of the scenarios. The modelling framework combines a database with a graphical programming interface. The database allows the management of both the input parameters and the simulation output for the different scenarios calculated. The graphical interface allows the definition of the structure of the modelled system and the quantitative interdependences between the individual structural elements at different structural depths.

The scope of the scenario model allows the increasing electrification processes in the heating and transport sectors to be considered, such as electric vehicles, electric boilers, heat pumps, and hydrogen use. Co-generation in different sectors is also explicitly represented in the model. The EM is implemented in this framework and Figure 3.6 gives an overview of its structure.

Details of the structure and relevant model equations were also recently described by Simon et al. (2018). The model calculates the energy flows of a system on an

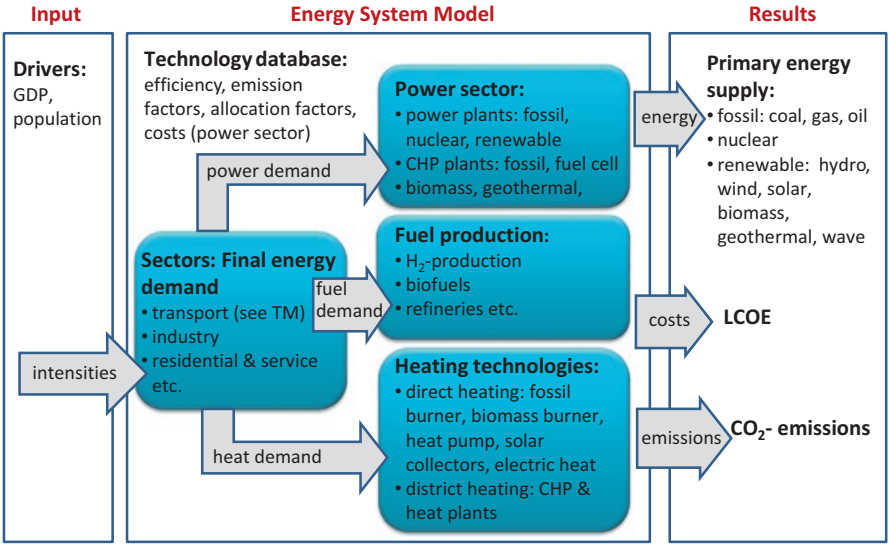

Fig. 3.6 Overview of the energy system model (EM) as implemented in Mesap/PlaNet

annual basis. These flows connect a set of technologies in each sector and for all relevant energy carriers, using linear equations. The equation system is solved sequentially and the model thus balances demand and supply. This approach is applied over the scenario period in 5-year steps until 2050. Ultimately, the overall final energy is calculated as described in the following equations:

$$FD_{ss}^{fe}(t) = \sum_{et} UED_{ss}(t) \cdot MS_{ss}^{et}(t) \cdot \eta_{fe}^{et}(t)$$

$$FD^{fe}(t) = \sum_{ss} FD_{ss}^{fe}(t)$$

$$TFD(t) = \sum_{fe} FD^{fe}(t) = \sum_{ss}\sum_{fe} FD_{ss}^{fe}(t) = \sum_{ss}\sum_{fe}\sum_{et} UED_{ss}(t) \cdot MS_{ss}^{et}(t) \cdot \eta_{fe}^{et}(t)$$

with:

- $FD_{ss,}^{fe}(t)$: demand of (final) energy carrier *fe* in sub-sector *ss*[1] at time step *t* [PJ/year]
- $FD_{ss,}^{fe}(t)$: total demand of (final) energy carrier *fe* at time step *t* [PJ/year]
- TFD(t): total final energy demand at time step *t* [PJ/year]

[1] The sub-sectors include 'heat' and 'non-heat electrical appliances' in the sectors 'Industry' and 'Residential and other', aviation, road transport, navigation, rail transport, non-energy consumption, the conversion sector, and storage and transmission losses for power and district heat. Conversion losses are taken into account in the calculation of the primary energy demand.

- $UED_{ss}(t)$: useful energy demand / transport services in sub-sector *ss* at time step *t* [PJ/year]
- $MS_{ss}^{et}(t)$: market share of end-sector technology *et* in sub-sector *ss* [dimensionless]
- $\eta_{fe}^{et}(t)$: efficiency of end-sector technology *et* using energy carrier *fe*[2] at time step *t* [dimensionless]
- *t*: time step

The indices denote:

ss: sub-sector
fe: (final) energy carrier
et: end-sector technology

The primary energy demand (without exports) is calculated as follows:

$$PD^{pe}(t) = \sum_{ct}\sum_{fe} FD^{fe}(t) \cdot MS_{fe}^{ct}(t) \cdot \eta_{fe}^{ct}(t)$$

$$TPD(t) = \sum_{pe} PD^{pe}(t)$$

with

- $PD^{pe}(t)$: total demand of (primary) energy carrier *pe* at time step *t* [PJ/year]
- TPD(t): total primary energy demand at time step *t* [PJ/year]
- $MS_{fe}^{ct}(t)$: market share of conversion technology *ct* in the generation of final energy carrier *fe* [dimensionless]
- $\eta_{fe}^{ct}(t)$: efficiency of conversion technology[3] *ct* using the final energy carrier *fe* at time step *t* [dimensionless]

The indices denote:

- *pe*: (primary) energy carrier
- *ct*: conversion sector technology[4]

The drivers of energy consumption include forecasts of population growth, gross domestic product (GDP), and energy intensities. Specific energy intensities are assumed for:

- electricity and heat consumption per person and per GDP;
- the ratio of industrial heat demand to GDP;

[2] Note that some technologies (e.g., electric heat pumps) require two energy carriers as inputs (electricity and environmental heat), with a specific efficiency for each energy carrier.

[3] Some conversion technologies produce more than one output, e.g. CHP plants, leading to constraints on efficiencies or market shares.

[4] Power and district heat generation, biofuel, synfuel, and H_2 generation, and refineries.

- demand for energy services, such as useful heat;
- different transport modes based on the Transport Model (see Sect. 3.4).

The model consists of a broad technology database across the heat, fuel, and power sectors, including sector coupling via combined heat and power (CHP), power-to-heat, and power-to-fuels technologies, and electric mobility.

For both heat and electricity production, the model distinguishes between different technologies, characterized by their primary energy sources, efficiency, and costs. Examples include biomass or gas burners, heat pumps, solar thermal and geothermal technologies, and several power-generation technologies, such as PV, onshore and offshore wind, biomass, gas, coal, nuclear, and CHP. In the transport sector, the model is directly linked to the results of the transport model (Sect. 3.3). For each technology, the market share with respect to total heat or electricity production is specified according to a range of assumptions, including targets, potential costs, and societal, structural, and economic barriers. The model eventually calculates the annual energy flows for a set of energy carriers.

The main inputs of the Energy System Model are:

- IEA World Energy Balances 2017 (IEA 2016a) for the calibration of the model for each world region in the years 2005–2015;
- IEA World Energy Outlook 2016/2017 (IEA 2016b, 2017a) for the parameterization of the model for the reference case (5.0 °C Scenario);
- various studies and statistics used for the assumption of further specific values, such as the power-to-heat ratios of co-generation plants, coefficients of performance of heat pumps, and the efficiency of hydrogen electrolysers and synthetic fuel production plants;
- narratives and assumptions regarding the further development of demand and supply technologies in line with the climate targets and by taking into account RES potentials and costs, stable market developments, and the constraints imposed by production capacities and regional implementation. These assumptions and narratives are described in detail in Chap. 5, Sect. 4.

The main outputs of the model are:

- the final and primary energy demands, broken down by fuel, technology, and energy sectors, as defined by the International Energy Agency (IEA)—industry, power generation, transport, and other (buildings, forestry, and fisheries);
- the results broken down by the three main types of energy demand—electricity, heating, and mobility (transport); specifically, the energy required, technology deployment, and financial investment for each of these energy demand types;
- total energy budget, which is the total cost of energy for the whole power system;
- energy-related CO_2 emissions over the projected period.

3.5 [R]E 24/7 (UTS-ISF)

The long-term scenarios calculated with the EM for 2020, 2030, 2040, and 2050 (see Sect. 3.4) are used as the input data for the dispatch modelling described in this section. The [R]E 24/7 model transforms a long-term scenario for a specific year into hourly load and generation curves. The annual electricity demand is transformed into an hourly load curve (see Sect. 3.2) and the annual power generation is transformed into a generation time series for variable power generation from regional solar and wind data and dispatchable power-generation data via interchangeable dispatch orders (see Sect. 3.7). The [R]E24/7 model is an accounting framework used to calculate the complete power system balance at 1 h resolution, and consists of two modules:

1. a flow calculation module, which balances the energy supply and demand; and
2. a cost calculation module, which calculates the corresponding generation and fuel costs.

The [R]E 24/7 model examines the influence of the dispatch order of power-generation technologies, the storage technologies, and the interconnection of up to eight regions. It calculates the impact of these variables on the overall system costs. [R]E 24/7 also calculates load curves for the residential, industry, and transport sectors based on the sector-specific energy intensity factors and applications that are in use. The factors and applications used depend on the GDP and population (see Sect. 3.2).

3.5.1 [R]E 24/7—Model Structure

Teske (2015) has developed a three-level grid model called '[R]E 24/7' as a grid analysis tool that differentiates between four voltage levels. For this analysis, the model has been simplified to eight interconnected clusters to reduce the data volume and the calculation time. High resolution, with multiple voltage levels, is impractical for a global energy scenario, because the required input data would not be available for all regions and—if the data were available—the calculation time would be extremely long. Therefore, the simplified [R]E 24/7 model uses eight clusters that can exchange electricity on an hourly basis with a user-defined interconnection capacity (see Sect. 3.8). Different voltage levels are not calculated. Figure 3.7 provides an overview of the different modules of the [R]E 24/7 model. In the first step, a database provides the main input data for the base year, including socio-economic parameters, the currently available power generation, and the energy infrastructure. The data are partly with the GIS tool (see Sect. 3.2) and partly from other information resources, such as publicly available databases of populations (UN PD DB 2018), GDP (CIA 2018; ST 7-2018), and energy efficiency indicators (WEC 2018),

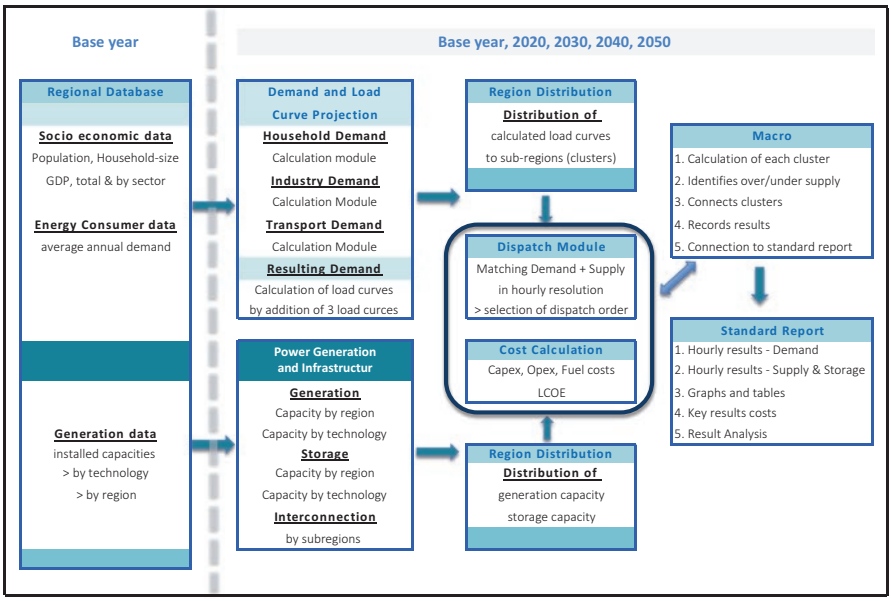

Fig. 3.7 Schematic representation of the [R] E24/7 model structure

and statistical data on renewable power generation from IRENA (REN21-GSR 2018) and the World Resources Institute (WRI 2018).

3.5.2 Development and Calculation of Load Curves

Energy demand projections and the calculation of load curves are important factors in calculating supply security and the dispatch and storage capacities required, especially for energy supply concepts with high proportions of variable renewable power generation. The [R]E 24/7 model calculates the development of the future power demand and the resulting possible load curves, because:

(a) Actual demand curves are not available for all countries and/or regions and are sometimes classified information.
(b) Future load curves with high penetration of storage, electric heating systems and electric mobility will have a very different shape than current load curves.
(c) For developing countries with low access to energy rates or little access to sufficient data, the curves must be calculated based on a set of assumptions because actual curves are neither available nor representative of future load curves.

The model generates load curves and the resulting annual power demands for three different consumer groups/sectors:

- households;
- industry and business; and
- transport (public and individual electric mobility).

Although each sector has its specific consumer groups and applications, the same set of parameters is used to calculate load curves:

- electrical applications in use;
- demand pattern (24 h);
- efficiency progress (base year 2015) for 2020 until 2050, and individual efficiency input for each year.

The calculations involve detailed bottom-up projections of the increased use of electricity for heating in buildings, for industrial process heat, for electric mobility, and for the production of synthetic fuels and hydrogen. They also include increased access to energy in developing countries based on the applications used, the demand patterns, and the household types. This allows detailed demand projections to be made.

Infrastructure needs, such as power grids combined with storage facilities, require in-depth knowledge of local loads and generation capacities. In this project, the annual electricity demand for each of the 10 world regions was calculated with the long-term EM. The [R]E 24/7 model breaks each region into up to eight subregions (or clusters) to calculate hourly load and generation curves.

3.5.3 Load Curve Calculation for Households

The model differentiates nine household groups, with various degrees of electrification and equipment:

- Rural—phase 1: Minimal electrification stage
- Rural—phase 2: White goods are introduced and increase the overall demand
- Rural—phase 3: Fully equipped western-standard household with electrical cooking and air conditioning and electric vehicle(s)
- Urban single: Single-person household with minimal equipment
- Urban shared flat: 3–5 persons share one apartment; fully equipped western household, but without electric vehicles
- Urban—Family 1: 2 adults and 2–3 children; middle income, middle western standard
- Urban—Family 2: 2 adults and > 3 children and/or higher income, full western standard
- Suburbia 1: average family, middle income, full equipment, high transport demand due to extensive commuting
- Suburbia 2: High-income household, fully equipped, extremely high transport demand due to high-end vehicles and extensive commuting

The following electrical equipment and applications can be selected:

- Lighting: 4 different light bulb types (LED, three efficiency classes of CFLs),
- Cooking: 10 different cooking stoves (2+4 burners, electricity, gas, firewood)
- Entertainment: 3 different efficiency levels of computers, TV, and radio types
- White goods: 2 different efficiency levels each for washing machine, dryer, fridge, freezer
- Climatization: 2 different efficiency levels each for fan, air-conditioning
- Water heating: A selection of direct electric, heat-pump, and solar heating systems

3.5.4 Load Curve Calculation for Business and Industry

The industrial sector is clustered into eight groups based on widely used statistical categories:

- Agriculture
- Manufacturing
- Mining
- Iron and steel
- Cement industry
- Construction industry
- Chemical industry
- Service and trade

Each sector has a definite energy intensity in energy per dollar GDP (MJ/$\$_{GDP}$), which is been converted to electrical units (kW/$\$_{GDP}$) based on an estimated fuel efficiency factor, electricity shares, and operational hours per year. The calculated electricity intensity per dollar GDP conversion can only show the required connected load and the specific consumption of an industrial sector to a first approximation because there is a variety of uncertainty factors, such as:

(a) significant regional differences;
(b) significant demand differences within one industry sector, such as *manufacturing* or *chemical industry*;
(c) lack of standardized data on industry energy demands, especially for the electricity sector.

Despite the high degree of uncertainty, we decided to apply this methodology because after an initial calibration, the current statistically recorded industrial electricity consumption in some well-documented countries (e.g., USA) and regions (e.g., Europe) can be recalculated with a tolerance of ± 10%. However, this methodology requires further research.

3.5.5 *Load Distribution by Cluster*

The spatial concept of the [R]E 24/7 is shown in Fig. 3.8. The model calculates the load distribution for one region, which can be broken down further to a maximum of eight sub-regions (or 'clusters'). Therefore, the 10 world regions modelled in this analysis are calculated separately. OECD North America, for example, includes Canada, USA, and Mexico. These three countries can be subdivided into up to eight clusters. A cluster can be a country (e.g., Mexico), a province/state of a country (e.g., Alaska), or a selection of several provinces/states (e.g., West Canada = British Columbia, Alberta, Yukon Territory, and North-West Territories). A cluster is defined to capture the existing interconnected power supply areas of a region, a country, or across several provinces. In Europe, for example, one cluster is the Iberian Peninsula (Spain and Portugal), a region within Europe that has only very limited interconnection with the central European grid system (UCT-E). However, data availability and the model limitations (maximum of eight clusters) force simplifications, and countries or state/provinces must be bundled together in one cluster even though they may have significant differences. Therefore, further research is required to obtain more detailed results for selected countries or provinces.

The distribution of the regional load, calculated in Sects. 3.3 and 3.4, is connected to the projected GDP, population, and power plant capacities for each cluster.

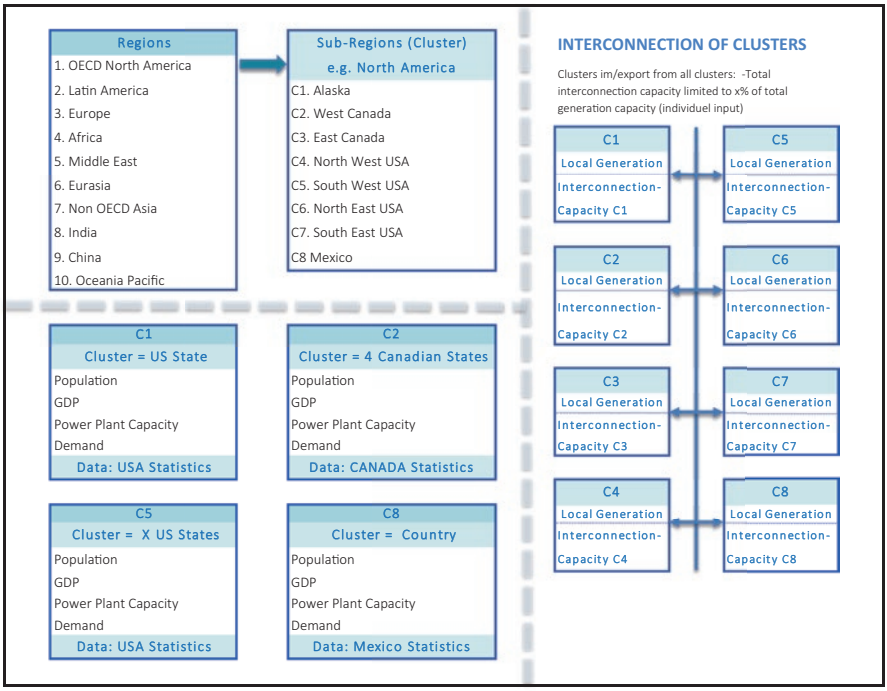

Fig. 3.8 Spatial concept of the [R]E 24/7 model

The cluster-specific data for the base year (2015) are taken from the model's database interface to calculate the demand and supply for the base year. When data are not available for each sub-region, the input data from the entire region will be broken down (in percentages) by cluster, according to the population—as a result of the GIS analysis. For the global analysis, the spatial distribution of the population, GDP, and power plant capacities remain unchanged over the modelled years (2020–2050) for all 10 regions and their respective sub-regions. In the next step, the resulting population and GDP values for each cluster are multiplied by the normalized load curves calculated as described in Sects. 3.3 and 3.4. Each cluster has an hourly load curve over one entire year (8760 h). Thus, one region (e.g., OCED North America) has eight different load curves.

3.5.6 The [R]E 24/7 Dispatch Module

Although the dispatch module for the [R]E 24/7 energy access model has been developed specifically for this study, integral parts have been taken from a model developed to analyse the generation and storage needs for a micro grid on Kangaroo Island (Dunstan and Fattal 2016), the Australian Storage Requirements (Rutovitz and James 2017), and a 100% Renewable Energy Analysis for Tanzania (Teske and Morris 2017). The key objective of this modelling is to calculate the theoretical generation and storage requirements for energy adequacy in each cluster and for the whole survey region (Tables 3.2 and 3.3).

Figure 3.9 provides an overview of the dispatch calculation process for one cluster. The key inputs include the generation capacities by type, the demand projections and load curves for each cluster, the interconnection with other clusters, and the meteorological data from which to calculate the solar and wind power genera-

Table 3.2 Input parameters for the dispatch model

Input parameter		
$L_{Cluster}$	Load Cluster	[MW]
$L_{Interconnection}$	Load Interconnection (Im- or Export)	[MW]
$L_{Initial}$	Initial Load (Cluster + Interconnection)	[MW]
$Cap_{Var.RE}$	Installed capacity *Variable Renewables*	[MW]
$Meteo_{Norm}$	Meteorological data for solar and wind	[MW/MW_{INST}]
$L_{Post\_Var.RE}$	Load after *Variable Renewable* Supply	[MW]
$Cap_{Storage}$	Capacity *Storage*	[MW]
$CapFact_{Max\_Storage}$	Max capacity factor storage technologies	[h/year]
$L_{Post\_Storage}$	Load after *Storage* Supply	[MW]
$Cap_{Dispatch}$	Capacity *Dispatch Power Plants*	[MW]
$CapFact_{Max\_Dispatch}$	Max capacity factor *Dispatch Power Plants*	[h/year]
$L_{Post\_Dispatch}$	Load after *Dispatch Power Plant* Supply	[MW]
$Cap_{Interconnection}$	Capacity *Interconnection*	[MW]

Table 3.3 Output parameters for the dispatch model

Output parameter		
$L_{Initial}$	Initial Load (Cluster + Interconnection)	[MW]
$L_{Post\_Var.RE}$	Load after *Variable Renewable* Supply	[MW]
$S_{EXECC\_VAR.RE}$	Access supply Renewables	[MW]
$L_{Post\_Storage}$	Load after *Storage* Supply	[MW]
$S_{Storage}$	Storage Requirement/Curtailment	[MW]
$CapFact_{Actual\_Storage}$	Utilization Factor Storage	[h/year]
$L_{Post\_Dispatch}$	Load after *Dispatch Power Plant* Supply	[MW]
$S_{Dispatch}$	Dispatch Requirement	[MW]
$CapFact_{Actual\_Dispatch}$	Utilization Factor *Dispatch Power Plants*	[h/year]
$L_{Post\_Interconnection}$	Load after *Interconnection* Supply	[MW]
$S_{Interconnection}$	Interconnection Requirement	[MW]
$CapFact_{Actual\_Interconnection}$:	Utilization Factor *Interconnection*	[h/year]

tion at hourly resolution. The calculation of one region with eight sub-regions will require eight calculation intervals. Table 3.4 shows the four different supply technology groups: variable renewables, dispatch power plants, storage technologies, and interconnections. The model allows the order in which the technology groups will be utilized to be changed to satisfy the demand. Storage and interconnection cannot be selected as the first supply technology. Within each technology group, the dispatch order can be changed. Tables 3.5, 3.6, and 3.7 provide an overview of all the available technologies and examples of different dispatch scenarios. While CSP plants with storage are dispatchable to some extent—depending on the storage size and the available solar radiation—they are part of the variable renewable group in the [R]E 24/7 model. Although the model allows the dispatch order to change, the 100% renewable energy analysis always follows the same dispatch logic. The model identifies excess renewable production, which is defined as potential wind and solar PV generation greater than the actual hourly demand in MW during a specific hour. To avoid curtailment, the surplus renewable electricity should be stored with some form of electric storage technology or exported to a different cluster. Within the model, the excess renewable production accumulates through the dispatch order. If storage is present, it will charge the storage within the limits of the input capacity. If no storage is present, this potential excess renewable production is reported as 'potential curtailment' (pre-storage).

Limitations: It is important to note that the calculation of possible interconnection capacities for transmission grids between sub-regions does not replace technical grid simulation. Grid services, such as inductive power supply, frequency control, and stability, should be analysed, although this is beyond the scope of this analysis. The results of [R]E 24/7 provide a first rough estimate of whether the increased use of storage or increased interconnection capacities or a mix of both will reduce systems costs.

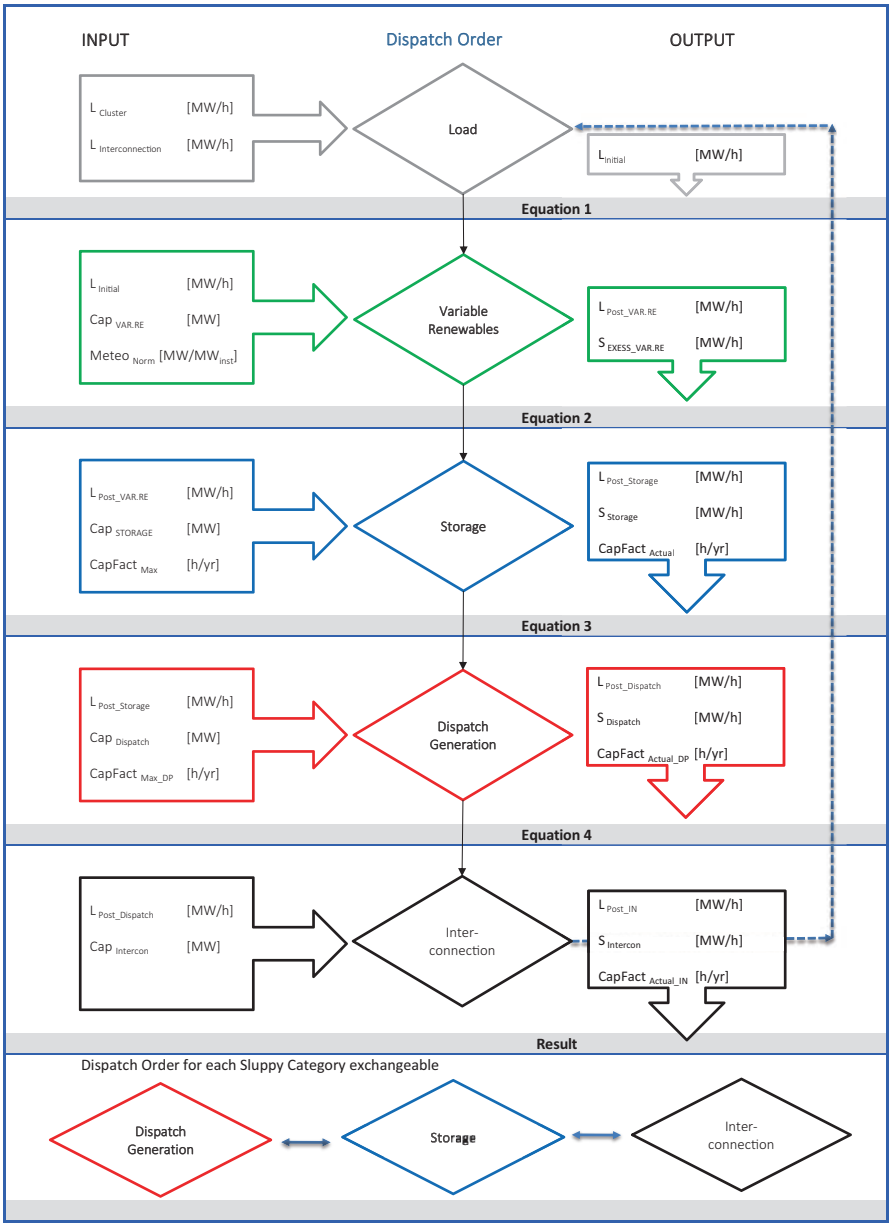

Fig. 3.9 Dispatch order module of the [R]E 24/7 model

Table 3.4 Technology groups for dispatch order selection

Technology options	Input
Variable renewables	Variable renewables
Storage	Storage
Dispatch generation	Dispatch generation
Interconnector	Interconnector

Table 3.5 Technology options—variable renewable energy

Variable renewable power technology options	Input
Photovoltaic—roof top -	Photovoltaic—roof top
Photovoltaic—utility scale -	Photovoltaic—utility scale
Wind—onshore -	Wind—onshore
Wind—offshore -	Wind—offshore
CSP (Dispatchable)	CSP

Table 3.6 Technology options—dispatch generation

Dispatch generation	
Technology options	Input
Bioenergy	Hydropower
Geothermal	Bioenergy
Hydropower	CoGen Bio
Ocean	Geothermal
Oil	CoGen Geothermal
Gas	Ocean
CoGen bio	Gas
CoGen geothermal	CoGen Gas
CoGen gas	Coal
CoGen coal	CoGen Coal
Coal	Brown Coal
Brown coal	Oil
Nuclear	Nuclear

3.5.7 Meteorological Data

Variable power-generation technologies are dependent on the local solar radiation and wind regimes. Therefore, all installed capacities of this technology group are connected to cluster-specific time series. The data were derived from the database *Renewable Ninja* (RE-N DB 2018), which allows the simulation of the hourly power output from wind and solar power plants at specific geographic positions throughout the world. Weather data, such as temperature, precipitation, and snowfall, for the year 2014 are also available.

Table 3.7 Technology options—storage technologies

Storage	
Technology option	Input
Battery	Battery
Hydro pump STORAGE	Hydro Pump storage
H2	H2

To utilize climatization technologies for buildings (air-conditioning, electric heating), the demand curves for households and services are connected to the cluster-specific temperature time series. The demand for lighting is connected to the solar time series to accommodate the variability in lighting demand across the year, especially in northern and southern regions, which have significantly longer daylight periods in summer and very short daylight periods in winter.

3.5.7.1 Solar and Wind Time Series

For every region included in the model, hourly output traces are utilized for onshore wind, offshore wind, utility solar, CSP, and roof-top solar energies. Given the number of clusters and the geographic extent of the study, and the uncertainty associated with the prediction of the spatial distribution of future generation systems, an representative site was selected for each of the five generation types. For utility solar and CSP, the indicative sites were situated in areas of high solar output, close to the transmission network or regional centre or city, and in areas without competing land uses (as described in the mapping methodology). A roof-top solar indicative site was chosen in the demographic centre of the region, usually the capital city.

The onshore wind indicative site selected for each region was situated in an area of non-competing land use with the highest average wind speed and close to the transmission network or regional centre or city. The offshore wind indicative site was an area within 100 km of the shore with the highest average wind speed, and close to the transmission network or regional centre or city. In some cases, no acceptable wind area within a region was available, in which case the wind potential was set to zero.

Once the indicative sites were chosen, the hourly output values for typical solar arrays and wind farms were selected using the database of Stefan Pfenninger at ETH Zurich and Iain Stafell (Renewables.ninja; see above). The model methodology used by the Renewables.ninja database is described by Pfenninger and Staffell (2016a, b), and is based on weather data from global reanalysis models and satellite observations (Rienecker and Suarez 2011; Müller and Pfeifroth, 2015; SARAH 2018). It was assumed that the utility solar sites were optimized, and as such, a tilt angle was selected within a couple of degrees of the latitude of the indicative site. For roof-top solar, this was left at the default 35° because it is likely that the panels matched the roof tilt.

The wind outputs for both onshore and offshore wind were calculated at an 80 m hub height because this reflects the wind data sets used in the mapping exercise. Although onshore wind and offshore wind are likely be higher than this, 80 m was considered a reasonable approximation and made our model consistent with the mapping-based predictions. A turbine model of Vestas V90 2000 was used.

Limitations: The solar and wind resources can differ within one cluster. In some cases, there are even different climate zones within one large cluster, e.g., in Australia and Russia. Therefore, the potential generation output can vary within a cluster and across the model period (2020–2050). Furthermore, some clusters extend significantly across several time zones, such as Russia. The model can only take into account the time variations in sunrise and sunset between different clusters, but not within a single cluster. The effect of time differences within clusters with a large east–west spread requires high-resolution modelling, which is possible with the [R]E 24/7 model but beyond the scope of this research project.

3.5.8 Interconnection Capacities

The interconnection capacities are set as a function of the total generation capacity within a cluster and a manually set percentage. Defining the relevant percentage of a country's overall (peak) capacity and/or total generation capacity is based on European energy policy. The European Union (EU) proposed in 2002 that all EU member states must establish a transmission capacity of at least 10% of the peak demand (in megawatts) by 2005 (EMP-BARCELONA 2002). The EU developed this regulation further, improved the calculation method, and increased the target to 15% (EU-EG 2017), whereas the [R]E 24/7 model implements a simplified approach by taking a percentage of the overall installed capacity. Clusters that are not connected at all to the real energy market (e.g., South Korea, Japan, Australia, and New Zealand in the OECD Pacific region) are assigned 0% interconnection capacity. Responsibly well-connected clusters (such as the south-western USA) are set to 15%, and highly interconnected countries (such as Denmark) are assigned up to 40%.

Several simplifications have been made to the [R]E 24/7 model for ease of computation and to accommodate the paucity of data and uncertainty about the future when designing the interconnector algorithms:

- Interconnections between the project-defined regions are the only ones considered, so all intra-regional interconnections or line constraints are excluded ('*copper plate*');
- Optimal load flow is neglected because policy and price signals are considered to be the factors dominating the international and inter-regional load flow;
- Non-adjacent inter-regional interconnections are neglected for computational reasons, e.g., one region cannot buy power from a region with which it does not share a border.

The algorithm devised for the function of the interconnectors is based on three key pieces of information for each region in a cluster:

– Excess generation capacity;
– Unmet load;
– Interconnection capacity with each adjacent region, both in and out.

The excess generation capacity and unmet load were calculated by running the model without the interconnectors to determine the excess or shortfall in generation when the load within the region is met. These excesses and shortfalls were calculated at the point in the dispatch cascade at which the interconnectors provide or consume power, for example, after the variable renewables and dispatchable generators and before the storage elements.

The interconnection capacity between adjacent regions was defined based on a percentage of the maximum regional load. The capacity was defined in a matrix, both to and from every region to every other region. For non-adjacent regions, the capacities were set to zero. A priority order for each region to every other region was given, so that if the region had an unmet load, it would be served sequentially with the excess generation of the loads in their defined order.

For every hour and for every region in each cluster, the possible interconnection inflow or outflow for load balancing was calculated. Each region was considered in turn, and the algorithm attempted to meet the unmet load with excess generation by adjacent regions, keeping track of the residual excess load and interconnector capacities. Each region's internal load was met first, before its generation resources were considered for other interconnected regions.

Once the total inflow and outflow of the interconnectors were calculated, the hourly values were fed into the model once more at the position in the cascade to which they were assigned, and the model was run again to give the total system behaviour. For regions sending generation capacity to other regions, the interconnector element behaved as an increase in load, whereas for regions accepting power from neighbouring regions, the interconnector element behaved as an additional generator, from the model's perspective.

3.6 Employment Modelling (UTS-ISF)

Two of the key dimensions influencing the social and economic impacts of the transition from fossil-fuel to clean energy are the quantity and type of jobs that are lost and created. Currently, there are limited data on the volumes of jobs that will be lost and created within particular occupations and locations during the transition to clean energy. National statistical agencies classify and collect data on occupations within the fossil fuel sectors but not within the renewable energy sectors (ABS 2017). ISF has developed a model to estimate the volume of renewable energy jobs under different 100% global renewable energy scenarios (Rutovitz and Dominish 2015), and an increasing body of research is estimating the jobs created by

renewable energy. The following section provides an overview of the basic methodology. Based on this, UTS/ISF has developed this methodology further, as presented in Sect. 3.2.

3.6.1 Quantitative Employment Calculation

In 2015, the Institute for Sustainable Futures (ISF) at the University of Technology Sydney (UTS) developed a quantitative employment model that calculates employment development in the electricity, heating, and fuel production sectors for the analysis of future energy pathways (Rutovitz and Dominish 2015). Figure 3.10 provides a simplified overview of how the calculations are performed, based on Rutovitz (2015b). The main inputs for the quantitative employment calculations are:

for each calculated scenario, e.g., the 5.0 °C (Sect. 5.1.1) and 2.0 °C Scenarios (Sect. 5.1.2),

- the electrical and heating capacity that will be installed each year for each technology;
- the primary energy demand for coal, gas, and biomass fuels in the electricity and heating sectors;
- the amount of electricity generated per year from nuclear power, oil, and diesel.

for each technology:

- 'employment factors', or the number of jobs per unit of capacity, separated into manufacturing, construction, operation, and maintenance, and per unit of primary energy for fuel supply;
- for the 2020, 2030, and 2050 calculations, a 'decline factor' for each technology, which reduces the employment factors by a certain percentage per year. This reflects the fact that employment per unit decreases as technology efficiencies improve.

for each region:

- the percentage of local manufacturing and domestic fuel production in each region, to calculate the proportions of jobs in manufacturing and fuel production that occur in the region;
- the percentage of world trade in coal and gas fuels, and traded renewable components that originates in each region.

A 'regional job multiplier', which indicates how labour-intensive the economic activity is in that region compared with the OECD, is used to adjust the OECD employment factors when local data are not available. The figures for the increase in electrical capacity and energy use from each scenario are multiplied by the employment factors for each of the technologies, and then adjusted for regional

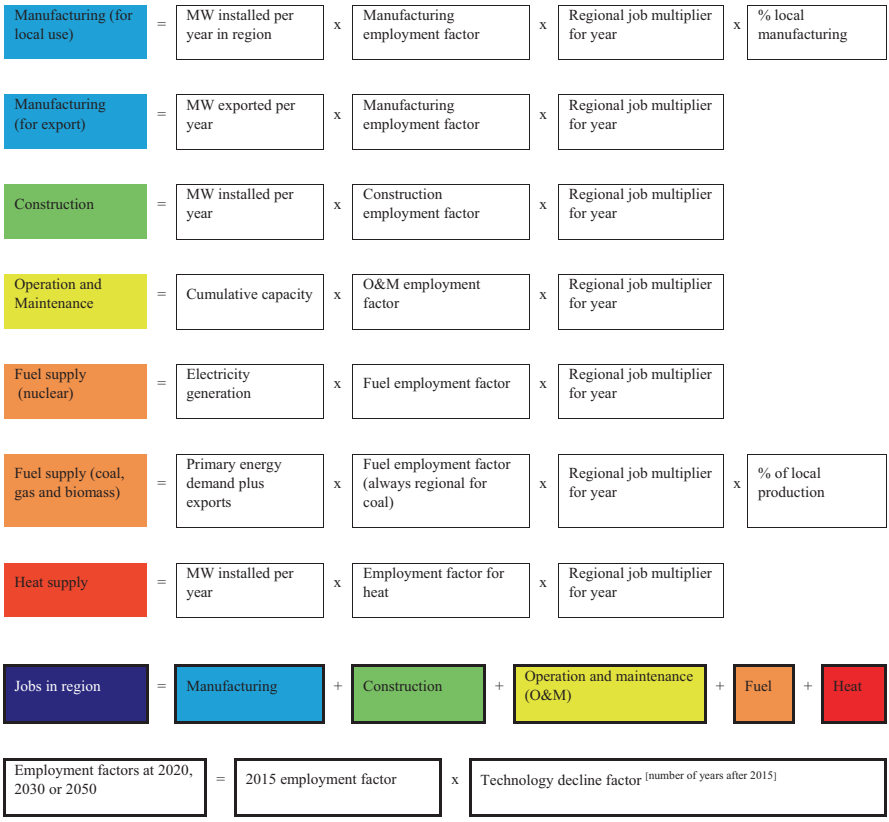

Fig. 3.10 Quantitative employment calculation: methodological overview

labour intensity and the proportion of fuel or manufacturing that occurs locally. The calculation is summarized in Fig. 3.10.

A range of data sources were used for the model inputs, including the International Energy Agency, US Energy Information Administration, BP Statistical Review of World Energy, US National Renewable Energy Laboratory, International Labour Organization, World Bank, industry associations, national statistics, company reports, academic literature, and the ISF's own research.

These calculations only take into account direct employment; for example, the construction team required to build a new wind farm. They do not include indirect employment; for example, the extra services provided in a town to accommodate the construction team. The calculations do not include jobs in energy efficiency because this is beyond the scope of this project. The large number of assumptions required to make these calculations means that employment numbers are only estimates, especially for regions where few data exist. However, within the limits of data availability, the figures presented are representative of employment levels under the 5.0 °C and 2.0 °C Scenarios.

3.6.2 Occupational Employment Modelling

The quantitative employment model documented in Sect. 3.6.1 were further developed to analyse the qualitative occupational composition of employment in the fossil fuel and renewable energy industries. UTS-ISF has developed a framework for modelling disaggregated occupational change, and this framework is described in this section.

Quantitative employment studies at the level of technology and project phases (manufacturing, construction, and O&M) are useful when providing estimates of aggregate job creation. However, more disaggregated, granular data on the locations and types of occupations are required to plan a just transition to renewable energy. For example, it is necessary to know how many electricians are currently employed in fossil fuel industries and how many will be employed in the renewable energy sectors. Although our forecasts will almost inevitably be wrong, key trends can be established. For example, we can direct our focus to areas of the workforce in which an increase in the supply of labour will probably be required, and to areas where the effects of dislocation will be greatest.

Using a variety of data sources, ISF has developed a framework for classifying and measuring job changes at different levels of occupational disaggregation, to provide a richer picture of the composition of this employment change. The methodology and key figures are detailed below.

Three primary studies that classify and measure the occupational compositions of renewable energy industries have been conducted by the International Renewable Energy Agency (IRENA). Using surveys of the participants in around 45 industries across a range of developed and developing nations, IRENA has estimated the percentages of person-days for the various occupations across the solar PV and onshore and offshore wind farm supply chains (IRENA 2017). Figure 3.11 is an example (in this case, for solar PV manufacturing).

IRENA's studies are the most detailed estimates available of the occupational compositions of the solar PV and onshore wind sectors. ISF has extended the application of IRENA's work. Chapter 10 provides more details about the methodology and the specific factors used in this analysis.

3.7 Material and Metal Resources Analysis (UTS-ISF)

3.7.1 Methodology—Material and Metal Resources Analysis

The future demands for metals have been modelled to better understand the resource requirements of the shift to renewable energy and transport systems. The future demands for metals have been modelled for the projection of 100% renewable energy and the full electrification of the transport system by 2050, as described in in Chap. 6.

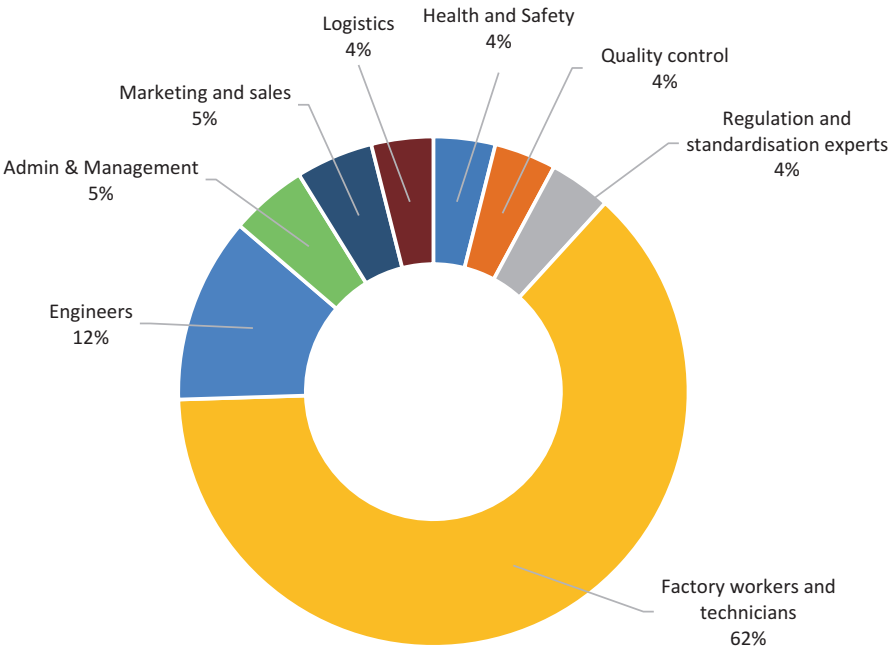

Fig. 3.11 Distribution of human resources required to manufacture the main components of a 50 MW solar photovoltaic power plant. (IRENA 2017)

The predicted demand for the metals required to produce clean energy each year is estimated based on the increase in capacity plus an additional amount required to replace the capacity or vehicles that reach the ends of their lives in each year (based on a lifetime distribution curve for the average lifetime). From this, the GW of capacity or number of vehicles introduced in each year is estimated (also accounting for the replacement stock for end-of-life technologies).

When assuming that the introduced amount of specific technologies in year t is l_t, the accumulated stock amount in year t (generation capacity or in-use stock) is S_t, and the discarded amount in year t is O_t, can be expressed by:

$$S_t = S_{t-1} + I_t - O_t \tag{3.1}$$

Where O_t depends on the number of use years of each product. This use year varies from product to product, and even within the same product group introduced into a society in the same year. The discarded year is not constant and has a lifetime distribution. Therefore, if the number of use years of the product is assumed as a, lifetime distribution can be defined as $g_{(a)}$. Hence, is given by following:

$$O_t = \sum_{a=0}^{a_{\max}} I_{t-a} g(a) \tag{3.2}$$

Where a_{max} is the maximum value of the product life. Therefore,I_t can be calculated with equation (3.3).

$$I_t = S_t - S_{t-1} + \sum_{a=0}^{a_{\max}} I_{t-a} g(a) \tag{3.3}$$

In this book, the Weibull distribution is used to consider the life characteristics of the products described above, with the key assumptions shown in Table 3.8.

Based on the annual introduced amount of clean energy technologies given by equation (3.3), the metal demand for technology p in year t is estimated as:

$$Demand_{p,t} = I_{p,t} \cdot Metal\ intensity_{p,t} \tag{3.4}$$

Where $Metal\ intensity_{p,t}$ is the amount of required metal in technology p in year t. Because this value can change over time with technological developments, we assume that the various scenarios incorporating the material efficiency improvement.

The demand estimated with equation (3.4) indicates the total metal requirements for the introduction of clean energy technologies. This demand arises from primary production (mined from natural deposits) and secondary production (recovered from end-of-life products). Secondary production could play an important role in the future by increasing metal availability and reducing the environmental impact. Therefore, we evaluated the effects of recycling by estimating the potential reduction in primary production entailed. When the recycling of end-of-life products is considered, primary production is given by equation (3.5).

$$Primary\ production_{p,t} = Demand_{p,t} - Discard_{p,t} \cdot Recycling\ rate_p \tag{3.5}$$

Where $Discard_{p,t}$ is end-of-life technology in year , and is estimated from the Weibull distribution, and the $Recycling\ rate_p$ indicates the proportion of metals recovered from end-of-life technology. Since this value can be increased by technological improvements, the metal price, and the amount of end-of-life product available, we assumed both the current recycling rate and an improved recycling rate.

This recycling rate is based on the rate of recycling of the metal within the technology (e.g., silver discarded from solar panels can be recycled into new solar panels), rather than as an average across the use of the metal, as has been done in previous studies. This has been chosen as the most appropriate recycling rate to use because we assume that by using recycling rates specific to the technology, it is more likely to offset demand for new materials for that technology.

Table 3.8 Key assumptions

Technology	Lifetime (years)	Shape parameter
Solar PV	30	5.38
Battery	8	3.5

Ultimately, the mineral requirements estimated with equations (3.4) and (3.5) under the various assumptions were compared with metal reserves and annual production (in 2017). A 'reserve' is regarded as the amount economically extractable with the current technologies and at the current metal price, and can change significantly over time. However, comparing reserves with estimated future requirements can provide insight into how the introduction of clean energy technologies will affect the physical availability of metals in the future. We also compared current production with the estimated future requirements to estimate the likelihood of a rapid increase in requirements. The key results are presented in Chap. 11.

3.8 Climate Model

3.8.1 Deriving Non-CO_2 GHG Pathways

This section provides an overview of the methodology that has been used to complement the energy-related CO_2 emission pathways for non-energy-related CO_2 emissions, other GHG emissions, and aerosols.

The energy-related CO_2 emissions were derived using energy-system modelling frameworks, but two different approaches have been used to derive the land-use CO_2 emissions and other GHG emissions. First, we will describe the approach that was used to determine other GHG emissions. This approach can be summarized as a statistical analysis of currently published scenarios. To derive non-CO_2 pathways that are consistent with the relevant emission mitigation levels, the non-CO_2 emissions were regressed against the fossil fuel and industrial CO_2 emissions. These regression characteristics were then used to derive the non-CO_2 emissions. This method has been newly developed in the context of this study and can be regarded as a further development of the Equal Quantile Walk method introduced by Meinshausen et al. (2006).

One challenge in applying the collective knowledge that is enshrined in multi-gas-emission scenarios in the literature is that regional and sectoral definitions differ slightly between the various modelling groups. Because most IPCC scenarios work are based on the emission categories used by the IAM community, their emission categories and regions have been adopted in this analysis of non-CO_2 emission pathways. The steps in the analysis are described in the following sub-sections.

3.8.1.1 Regional Definitions

First, the regional energy-related CO_2 emissions developed in the previous sections must be transformed to match the five Renewable Communities Program (RCP) regions used by the IAM community, into the regions OECD90 (OECD countries,

Table 3.9 Regional definitions according to the Integrated Assessment Modelling community

Regions	Developing Asia	Europe	Africa	Middle East	Central & South Amer	Eurasia	China	India	North America	OECD Asia Oceania	Subtotal
RCP5_Asia	1,561	-	-	-	19	21	8,826	1,985	-	674	13,086
RCP5_REF	-	720	-	-	-	2,153	-	-	-	-	2,873
RCP5_MAF	-	-	1,174	2,021	-	-	-	-	-	-	3,195
RCP5_OECD90	2	3,031	-	-	-	-	-	-	5,766	1,577	10,376
RCP5_LAM	-	-	-	-	1,216	-	-	-	461	-	1,676
Subtotal	1,563	3,751	1,174	2,021	1,235	2,174	8,826	1,985	6,226	2,251	31,206

membership status as of 1990), ASIA (Asian countries), REF (economies in transition), LAM (Latin America), and MAF (Middle East and Africa). Table 3.9 (above) indicates the overlap and differences between the RCP regions with the other regions described in this report. As an indicator of how different the regional definitions are, we used the fossil fuel and industrial emissions for the year 2015 according to the 2017 update of the PRIMAP database (Gütschow et al. 2016).

Table 3.9 provides an overview to the regional definitions used in this study. The top row indicates the regions for the CO_2 fossil and industrial emissions, and the various rows refer to the five regions used in IAMs. To derive the non-CO_2 emissions, we used the IAM's five RCP regions. The numbers indicate the fossil fuel and industrial emissions in the year 2015 in $MtCO_2$, aggregated from country-level data. The colour shading of the cells indicates where most of the 2015 emissions occurred.

Table 3.9 Regional definitions according to the Integrated Assessment Modelling community (so-called 'RCP5' regions) compared with the other regions used in this study The overlap and differences between the two sets of regional definitions are shown with the 2015 fossil and industrial CO_2 emissions. For example, the first row indicates that the largest sub-region in the RCP5_Asia group is China, with 8,826 $MtCO_2$ of emissions.

The transfer of the energy-related CO_2 emission results to fit the IAM's regional categorization (which is consistent with IEA WEO reports) was performed by first disaggregating all the results to country-level data. A simple proportional scale was applied to the 2015 energy-related country-level CO_2 emissions from the PRIMAP database. The disaggregated country-level data were then re-aggregated at the RCP5 regional level.

3.8.1.2 Harmonization: Emission Category Adjustments

Before proceeding with the application of CO_2 versus non-CO_2 statistical relationships, a harmonization step is necessary. Various IAM use slightly different categories, emission factors, and activity data to estimate emissions. This can result in

some spread in the current emission estimates for the same regions and categories. To address this issue, the standard practice in the IAM community is to work with harmonized emissions scenarios, meaning that the original emissions scenarios have either been scaled or shifted towards a common reference point. A recent historical emission level is normally chosen as this reference point. Here, we chose the 2015 emissions across the five RCP regions.

Harmonization was performed in two steps. First, emissions were added that were related to the CO_2 fossil and industrial emission categories (such as waste-related emissions) and that were outside the scope of emissions in the energy-related CO_2 emission chapters. The scenarios from which these 'other' energy-related CO_2 emissions were taken were: the SSP2_Ref_SPA0_V25_upscaled_MESSAGE_GLOBIOM (for the 5.0 °C reference scenario); SSP1_26_SPA1_V25_IMAGE (for the 2.0 °C Scenario), and SSP1_19_SPA1_V25_IMAGE scenario (for the 1.5°C Scenario). In the second harmonization step, the overall sum of the complemented 2.0 °C and 1.5 °C scenario CO_2 emissions were compared with the overall fossil and industrial sum of CO_2 emissions in the year 2015, which were used for scenario harmonization under the CMIP6 ScenarioMIP process (Meinshausen et al., in preparation). This comparison revealed that there were still differences between the complemented energy scenarios (see Chapter 8) and the harmonization emission levels for the various regions. These differences could again have resulted from different emission factors or activity assumptions, or they could simply reflect genuine uncertainty in the overall global and regional anthropogenic emissions. Consistent with the processing steps used in the CMIP6 process, we up- and down-scaled the raw and regionally disaggregated energy scenario emissions towards the harmonization emission levels. Figure 3.12 shows the differences between the raw emission scenario data, the data re-aggregated into the RCP regions, and the CMIP6 emission harmonization fossil and industrial CO_2 emission levels for 2015 (in GtC). The differences were bridged by applying a time-constant scaling factor.

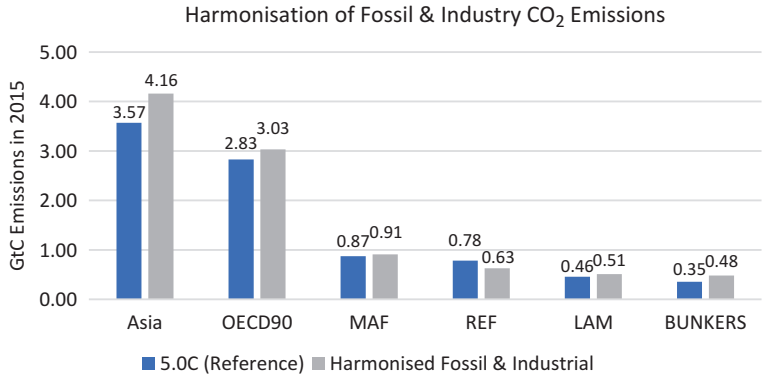

Fig. 3.12 Differences between the raw LDF emission scenario data

3.8.1.3 A New Quantile Regression Method for Non-CO_2 Gases

The completed fossil and industrial CO_2 emission time series can now be compared with the set of scenarios in the literature. In this study, we used 811 scenarios from CMIP6 databases or the databases underlying the IPCC SR1.5 report. These literature-reported studies are either reference scenarios or mitigation scenarios with a specific forcing target or climate target. Some of the scenarios aim for 1.5 °C levels of change, others for 450 ppm CO_2-equivalence concentrations, and yet others assume fragmented worlds, with regional rivalries and no consistent policy approach. In summary, the input assumptions of all these literature-reported scenarios vary widely, yet all have some formal energy-system modelling framework behind them that provides first-level assurance that the envisaged CO_2, methane, nitrous oxide, and other gas emission levels are not set below the limits considered technologically feasible under a certain set of boundary conditions, such as the requirement to continuing feeding the human population. The technological and economic feasibilities of emission pathways are fluid concepts, subject to change in response to technological advances and changes in policy settings.

This study and the approach it uses are not dependent on absolute levels of mitigation costs or precise definitions of technological feasibility. Instead, the method used assumes that that non-CO2 gases are reduced with a similar effort as that required to reduce CO_2 emissions. Therefore, using the emission characteristics from a large set of scenarios reported in the literature, we assume similar levels of technological feasibility, economic mitigation costs, and implementation opportunities will be required to reduce emissions of CO_2 and various other gases.

More specifically, we derived the non-CO_2 emissions in a particular year by ranking all the scenarios against the indicator of fossil and industrial CO_2 emissions in that year (see Fig. 3.11 below). By comparing them to the 'crowd' of other literature-reported scenarios, the LDF pathways could also be ranked. Specifically, the LDF reference scenario turned out to be around the 75th percentile of the distribution of the fossil and industrial CO_2 emissions across all 811 scenarios considered. By contrast, the lower 1.5 °C Scenario and 2.0 °C Scenario were not at the absolute lower boundary of the 811 scenario distribution, but were close to it. The 1.5 °C Scenario ranked between the zero and first percentile—that is, among the 1% most stringent scenarios in the literature for the years 2025–2045. In the period until 2050, the 2.0 °C Scenario was situated between the 5th and 10th percentiles of the scenario distribution (see Fig. 3.13).

Figure 3.13 shows the 1.5 °C and 2.0 °C Scenarios, their absolute fossil and industry CO_2 emissions until 2050 (upper panel), and their respective locations in the set of 811 literature-reported scenarios considered (lower panel). The post-2050 scenario extensions were extrapolated differently for fossil and industrial CO_2 and the non-CO_2 gases. To derive the non-CO_2 gases, the 2050 percentile location was assumed constant for the remainder of the twenty-first century. For the fossil and industrial CO_2 emissions in the 2.0 °C and 1.5 °C Scenarios, which do not assume

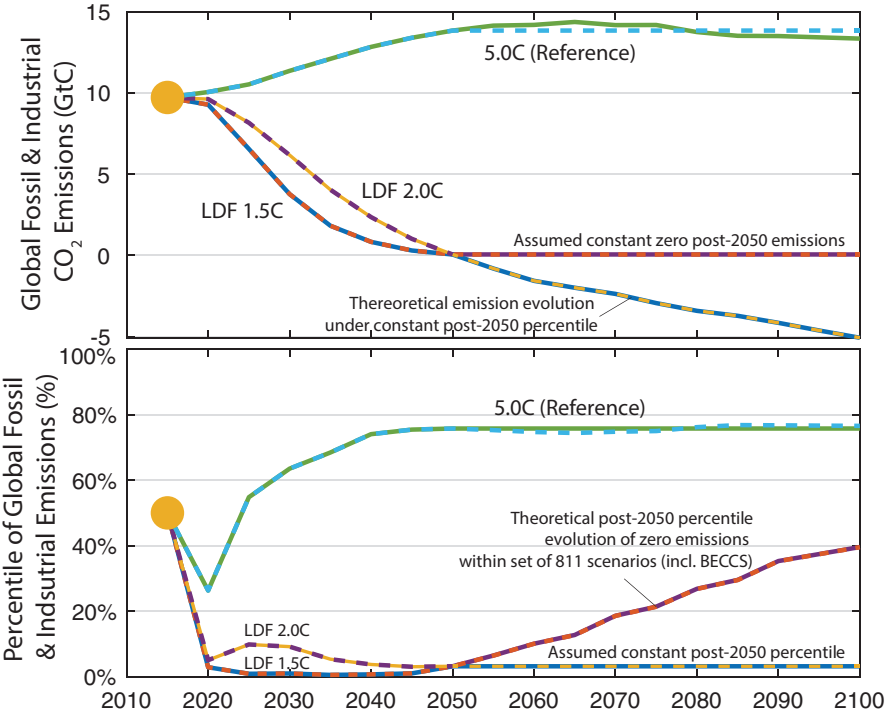

Fig. 3.13 The 2.0 °C and 1.5 °C scenarios and their absolute fossil and industry CO_2 emissions until 2050. The energy-related CO_2 emissions pathways from the other chapters are used until 2050, and then extended beyond 2050 by either keeping the CO_2 emissions constant (in the case of the 1.5 °C and 2.0 °C Scenarios, i.e., red and purple dashed lines beyond 2050 in the upper panel) or by keeping the percentile level within the literature-reported scenarios constant (in the case of the reference scenario, i.e., green solid line in the upper panel). The percentile rank within the other literature-reported scenarios is shown in the lower panel. The constant absolute emission level after 2050 in the case of the 1.5 °C and 2.0 °C Scenarios can be seen to result in an increasing percentile rank among all the literature-reported scenarios (increasing purple–red line in the lower panel)

BECCS to achieve net negative emission levels, a continuation of the constant zero emission level was assumed (straight constant emission level in the upper panel corresponding to the increasing percentile level of the red–blue dashed line in the lower panel).

3.8.1.4 'Pseudo' Fossil and Industrial CO_2 Extensions Beyond 2050

By the end of the century, almost 40% of all of 811 scenarios will feature net negative fossil and industrial CO_2 emissions, largely because there is some level of biomass and CCS deployment. Given that the energy scenarios developed for this study do not assume, by design, any BECCS-related emission uptake, the extended post-2050 energy scenarios are assumed to be consistent with other scenarios in which emissions will be around zero by the end of the century. However, those other

scenarios with zero emissions by the end of the century tend to reflect a much lower level of mitigation effort. Therefore, to derive non-CO_2 emissions that involve a level of effort that is comparable to the mitigation effort involved in reducing energy-related CO_2 emissions, we assumed that the energy scenarios developed for this study were comparable to other scenarios that share zero emissions around 2050. This percentile 'stringency' level was then held constant for the remainder of the twenty-first century. Therefore, whereas the actual fossil and industrial CO_2 emissions in the LDF scenarios are assumed to remain constant at zero, the non-CO_2 gas emissions are derived from data in the existing literature, as if the scenarios remained at a stringency level of ~3% in the second half of the twenty-first century (see the lower panel in Fig. 3.13).

We now have the fossil and industrial CO_2 emission levels throughout the twenty-first century for each of the three scenarios, and have complemented these with the 'pseudo' CO_2 emission levels for the second half of the twenty-first century. Therefore, we can derive the corresponding non-CO_2 emissions.

In the first step, we derived the total non-CO_2 emissions for a specific year and for the world as a whole. In the second step, we determined the shares of global fossil and industrial emissions versus the land-use-related emissions—again regressed against the overall fossil CO_2 emission level as an indicator of the 'stringency' of the scenario. In the third step, we disaggregated these fossil and land-use-specific emission time series into regional time series. Again, the shares of the regional emissions were derived with the same quantile regressions shown in Fig. 3.13 above. With these three quantile regression steps, we inferred either the lower (if lower quantile ranges are chosen), medium (for a median 50% quantile regression), or higher emission levels of the other gases. In this study, we do not intend to provide probabilistic emission scenarios and therefore limited our quantile regression choice to the median 50% setting for all regions, sectoral divisions, and other global total gases.

The major advantage of this newly developed method compared with the EQW method developed earlier (Meinshausen et al. 2006) is that the negative correlations between CO_2 and other gases can also be taken into account. By performing all quantile regressions in the space defined by the global fossil and industrial CO_2 emissions in a particular year, any kind of non-linear, positive or negative relationship with other non-CO_2 gas emission levels, sectoral divisions, or regional divisions are automatically incorporated into the final result—reflecting the overall characteristics of the chosen set of emission scenarios. Not all the 811 emission scenarios contained details of all the sectoral and regional divisions, but the stepwise approach of this method can incorporate the characteristics from all the scenarios in whatever detail is available.

Figure 3.14 shows sample distributions of the emission scenario characteristics for the year 2040 and a subset of 21 GHGs. The x-axis of each plot shows the global fossil and industrial CO_2 emissions, and the y-axis shows the global emission levels of another GHG, with one marker (blue dot) for each literature-reported scenario considered. The five red lines are quantile regressions at the levels of 20%, 33%, 50% (median), 66%, and 80% of the scenario distribution. It can be clearly seen that some total gas emissions correlate strongly with the fossil and industrial CO_2 emissions

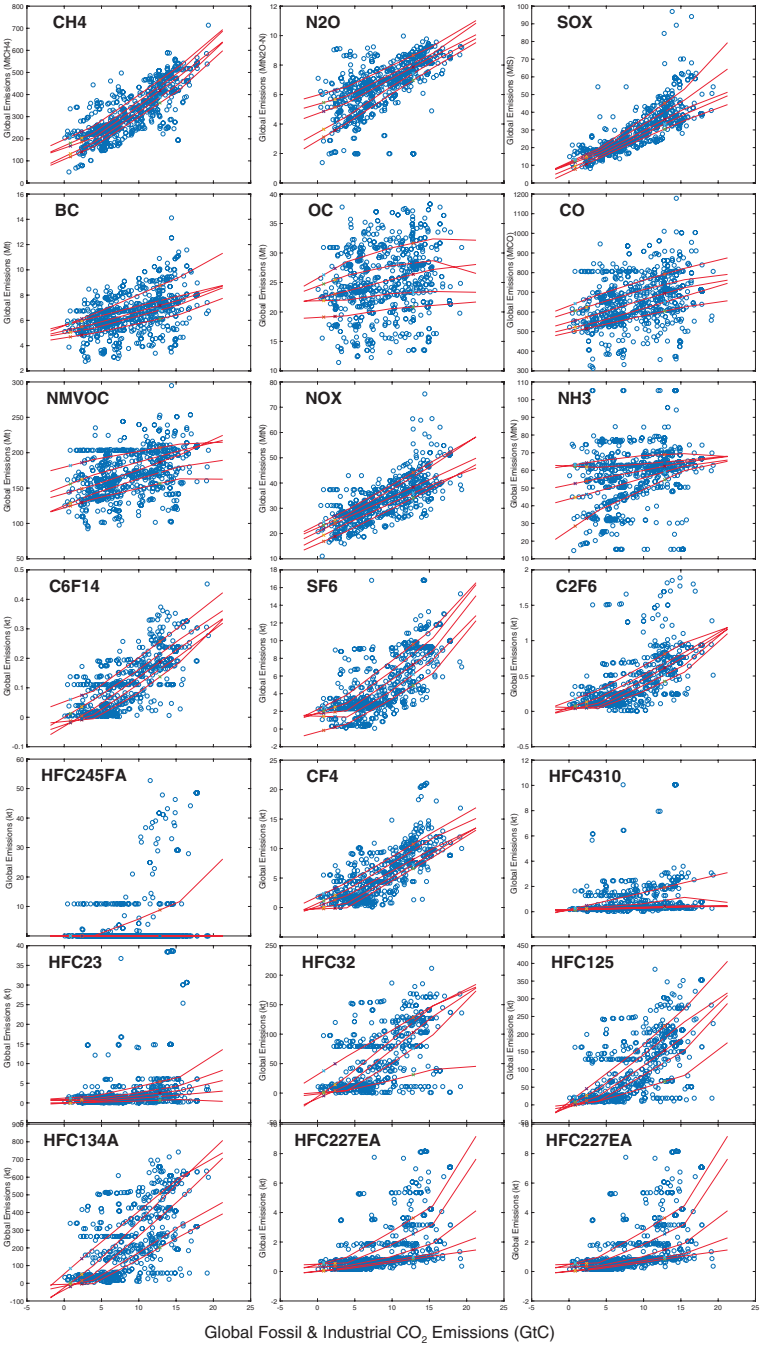

Fig. 3.14 Example distributions of emissions scenario characteristics

(such as the SO_X aerosols in the top-right panel), whereas others correlate less strongly. This method reflects the level of correlation in the finally derived multi-gas scenarios.

3.8.1.5 Land-Use Assumptions

In principle, the same methodological approach can be used for land-use emissions. In the IAM scenarios, the emission sequestration with the BECCS technology is reported as a negative emission in the fossil and industrial CO_2 emission categories. Therefore, the quantile regression approach can also be applied to the land-use CO_2 sector. However, to more explicitly define the land-use choices that are implied by various land-use scenarios, we developed a new (probabilistic) scenario in conjunction with another land-use emission project (Dooley et al. 2018)

This method is based on various literature-reported studies and we provide an overall synthesis of four different land-use-based sequestration pathways: 'forest ecosystem restoration', 'reforestation', 'sustainable use of forests', and 'agroforestry'. These land-use sequestration pathways are based on the premise that the better management of terrestrial ecosystems should allow previously degraded carbon stocks to be restored, entailing the removal of significant atmospheric CO_2 (DeCicco and Schlesinger 2018; Law et al. 2018; Mackey et al. 2013; Mackey 2014; Nabuurs et al. 2017). We derived the overall pathways separately for the temperate and boreal regions on the one side and the subtropical and tropical regions on the other. This distinction is largely consistent with the dominant distinction of different climate domain characteristics in the literature (Grace et al. 2014; Houghton and Nassikas 2018; Pan et al. 2011), although the temperate and boreal biomes are as different in terms of land-use and forest ecosystem characteristics as the tropical biomes are from each of them. However, we derived only two climate domains because several of the RCP regions cross both temperate and boreal biomes. A narrative for each of these pathways is available in Table 3.10 below.

Based on literature studies and Food and Agriculture Organization (FAO) statistics, we then defined the available areas (and their uncertainties) for each of the four sequestration pathways. Similarly, we sourced average estimates of the maximal annual sequestration rates for the biomes (and their levels of uncertainty) for those four sequestration pathways—again distinguished in the large temperate/boreal and subtropical/tropical climate domains. We assume that after a certain 'phase-in period', this maximal annual sequestration rate can be reached and sustained for a number of years. We assume that after some decades to centuries, the capacities of these terrestrial ecosystems as carbon sinks will slowly decline until they reach equilibrium, termed the 'saturation' period. At the equilibrium point, these ecosystems have a net zero effect on atmospheric CO_2 over the time scales of interest here (Houghton and Nassikas 2018). The period over which the maximal sequestration rate is assumed, is reduced by the half-length of the corresponding phase-in and phase-out periods to account for the cumulative carbon uptake in those periods. As the last element in this framework, we assume a cap on the median carbon density change that is achieved over the full period. The difference between a degraded for-

Table 3.10 Narrative for each sequestration pathway per climatic biome

Pathway	Climatic domain	Narrative
Forest ecosystem restoration (set aside areas of degraded natural forest to restore to primary forest—25% of total)	Te,B	Assume 25% of degraded natural forest put aside for full ecosystem and carbon stock recovery. Saturation times in temperate and boreal forests can be well over 100, or even 200 years (Luyssaert et al. 2008; Roxburgh et al. 2006). 25% set-aside is slightly higher than assumptions made in recent literature (Böttcher et al. 2018; Nabuurs et al. 2017), but in line with calls from conservation and indigenous movements.
	S,Tr	Assume 25% of degraded natural forests across the tropics set aside for full ecosystem and carbon stock recovery. Stopping all deforestation, wood harvest and temporary use, while traditional and customary uses continue. Net Primary Productivity (NPP) is higher across the tropics than in temperate and boreal biomes (Anav et al. 2015), hence sequestration rates are higher, but saturation times are shorter. We assume 60 years to ecosystem maturity (Arneth et al. 2017; Poorter et al. 2016). Sequestration rates across all biomes for forest ecosystem restoration are lower than post-logging recovery rates, as here we assume mixed age-class forests which have not been recently logged than (>20 years ago), which then saturates when forest reaches maturity.
Reforestation (forest expansion through natural regeneration)	Te	Forest expansion on recently deforested land via natural regeneration of forests (passive regeneration) or reforestation of mixed native species (assisted regeneration). Extent of forest expansion is assumed to occur in line with current political targets: 350 Mha of reforestation by 2030 under the Bonn Challenge. Further, this 350 Mha is assumed to be reforestation for conservation purposes, which creates an ongoing sink from 2030 to 2100, with saturation assumed at 100 years. Boreal areas excluded due to albedo effect (Houghton and Nassikas 2018).
	S,Tr	Natural forest expansion on recently deforested land as described above. We assume 80% of forest expansion occurs in the tropics, given 80% of Bonn Challenge pledges are in tropical regions (Wheeler et al. in press). All regeneration is assumed to be with natural forests rather than plantations, as this delivers the highest mitigation and biodiversity values (Grace et al., 2014; Wheeler et al. in press). Saturation of tropical regrowth forests is assumed at 60 years, although large trees can take well over a century to mature (Poorter et al. 2016).

(continued)

Table 3.10 (continued)

Pathway	Climatic domain	Narrative
Sustainable use of forests (secondary forests under continued (but reduced) forest harvest)	Te,B	Sustainable use of natural production forests (i.e. excluding plantations) under continued wood harvest. Multiple studies show the potential to double forest carbon stocks in production forests through reducing harvest intensity and extending rotation lengths (Law et al. 2018; Nabuurs et al. 2017; Pingoud et al. 2018). Wood harvest is slightly reduced, requiring reduced demand for wood products, more efficient wood use and compensation to land-owners (Law et al. 2018; Pingoud et al. 2018). Including harvested wood products (HWP) in calculations could increase mitigation values (Houghton and Nassikas 2018; Nabuurs et al. 2017), but the life-time of HWP is generally too short to realise mitigation value compared to residence times in forest biomass (Law et al. 2018; Keith et al. 2015).
	S,Tr	Reduced harvest intensity and management practices such as reduced impact logging have not been shown to increase carbon stock in tropical forests (Martin et al. 2015). Carbon stocks are concentrated in commercially-valuable hardwood trees taking >100 years to reach maturity; hence selective logging as practiced across the tropics significantly decreases standing carbon stocks (Lutz et al. 2018; Zimmerman and Kormos 2012). Our scenario assumes no commercial logging of tropical forests, and the extent of shifting cultivation is halved, allowing traditional practices to continue with lengthened fallow times and/or improved swidden practices (Mackey et al. 2018; Ziegler et al. 2012).
Agroforestry (Trees in croplands)	T,B	We calculate biome-average sequestration rates from the literature for above-ground carbon uptake due to a broad range of agroforestry practices (Watson et al. 2000; Nabuurs et al. 2017; Ramachandran Nair et al. 2009), and subtract from this the baseline increase observed by Zomer et al. (2016). We apply this uptake to 20% of permanent cropland, and assume the resulting sequestration rate could be sustained for 50 years (Watson et al. 2000).
	S,Tr	

These domains are defined as temperate (Te), boreal (B), subtropical (S), or tropical (Tr). Note, this narrative overlaps with another land-use-related study (Dooley et al. 2018)

est ecosystem and its natural carbon-carrying capacity is the maximum potential for additional sequestration. Therefore, we used biome-averaged values for the per hectare carbon density of undisturbed forest ecosystems (Keith et al. 2009), rather than average global biome values (Liu et al. 2015), to define the maximum carbon density. Although the LDF scenarios only extend to 2050 or to 2100 for all the other GHGs, we modelled the land-use sequestration pathway assumptions until 2300 to be able to apply the overall ‘added carbon density’ cap.

Our climate-domain- and sequestration-specific assumptions regarding the median values, their uncertainty ranges, and confidence intervals are given in

Table 3.11. Our method of combining these input assumptions is a basic Monte Carlo ensemble. Given the symmetry or asymmetry and respective confidence intervals of the factors provided, we then created normal, lognormal, or skewed normal distributions (the latter is a linear combination of the normal and lognormal distributions to achieve the desired skewedness). We then made 500 independent draws from all four factors considered (area, maximum sequestration rate, phase-in time, and phase-out time). We repeated that process independently for each sequestration pathway and for each country within each climate domain. The areas for each country within the climate domains were assumed to be proportionally distributed by the relevant 'FAO Scaling Area' (see third column in Table 3.11), so that the climate domain aggregate areas matched our input assumptions for the respective sequestration pathway.

After combining all the country-specific and sequestration-pathway-specific time series for carbon uptake per sequestration pathway, we then checked whether the resulting cumulative sequestration over time (specifically its median) was at or below the specified maximum for the median carbon density change per hectare. If it was not, we scaled all the country-specific results proportionally, so that the median matched the cap on the carbon density gain.

3.8.2 Model for the Assessment of GHG-Induced Climate Change

To compute GHG concentrations and the implications for radiative forcing, global mean temperatures, and global mean sea-level rise, we used the reduced-complexity 'Model for the Assessment of Greenhouse-gas-induced Climate Change' (MAGICC), as described by Meinshausen et al. (2011). The model has recently been extended by the addition of a newly designed sea-level rise module, as described in Nauels et al. (2016).

The MAGICC model has at its core an upwelling-diffusion ocean with 50 layers, in both the northern and southern hemispheres. Some simpler model approaches, with only a diffusive one-box ocean, for example, tend to overestimate the medium-term warming compared with the longer-term warming, (i.e., they tend to reach equilibrium too quickly). In the short term, the MAGICC modelling structure provides faster warming, but a lower approach to equilibrium, due to the effective cooling cycle that mimics the sinking polar ocean waters.

Although simple in its general structure, the MAGICC model uses a broad coverage of GHGs and aerosols. This is much broader than for earth system models, because it would be too computationally expensive to carry around tracers for every minute GHG concentrations of, say, HFC227EA. Because of the breadth of the GHGs that MAGICC can model, its calibrated carbon cycle, and its calibrated climate system with feedbacks and heat exchange parameterizations, it is frequently used as a climate model in IAMs. For example, the IMAGE and MESSAGE teams both have MAGICC inbuilt.

IPCC Assessment Reports also frequently use MAGICC as the modelling framework to determine the exceedance probabilities of various emission pathways. For

Table 3.11 Assumptions regarding the four land-use sequestration pathways for two climate domain categories

Pathway	Climatic domain (Te = Temperature; B = Boreal; S = Subtropical; Tr = Tropical)	FAO scaling area	Assumed available area (Mha)	Related sources	Assumed median added carbon maximum (MgC/h)	Assumed maximum sequestration rate (MgC/ha/year)	Related sources	Saturation period (Years)	Related sources	Phase in period (Years)	Phase out period (Years)
Forest ecosystem restoration (set aside areas of secondary forest to restore to primary forest—25% of total)	Te,B	Other Natural Forest Area 2015	276 (80%: 248–303)	FAO (2016)	185 (Keith et al. 2009)	0.5 (90%: 0.25–1)	Pan et al. (2011)	100 (80%: 70–130)	Luyssaert et al. (2008) and Roxburgh et al. (2006).	20 (90%: 7–20)	30 (90%: 10–100)
	S,Tr		335 (80%: 302–369)	FAO (2016)	172	1.1 (90%: 0.55–2.2)	Pan et al. (2011)	60 (80%: 42–78)	Pan et al. (2011), Grace et al. (2014), and Asner et al. (2018)	15 (90%: 7–20)	20 (90%: 10–100)
Forest expansion via reforestation (land-use change from non-forest to forest through natural regeneration)	Te	Change in total forest area from 1990 to 2015	50 (80%: 45–55)	FAO (2016)	185	2.62 (80%: 0.56–7.05)	IPCC (2006)	100 (80%: 70–130)	Roxburgh et al. (2006) and Luyssaert et al. (2008)	25 (90%: 7–20)	30 (90%: 10 to 100)
	S,Tr		300 (80%: 270–330)	FAO (2016)	172	3.1 (80%: 0.42–8.46)	IPCC (2006)	60 (80%: 42–78)	Pan et al. (2011), Grace et al. (2014), and Poorter et al. (2016)	20 (90%: 7–20)	20 (90%: 10 to 100)

(continued)

Table 3.11 (continued)

Pathway	Climatic domain (Te = Temperature; B = Boreal; S = Subtropical; Tr = Tropical)	FAO scaling area	Assumed available area (Mha)	Related sources	Assumed median added carbon maximum (MgC/h)	Assumed maximum sequestration rate (MgC/ha/year)	Related sources	Saturation period (Years)	Related sources	Phase in period (Years)	Phase out period (Years)
Sustainable use of forests (secondary forests under continued but reduced forest harvest)	Te,B	Production Forest 2015	743 (80%: 669–817)	FAO (2016)	185 (an upper end estimate, possibly too high, cf. Liu et al. 2015)	0.4 (80%: 0.36–0.44)	Nabuurs et al. (2017)	100 (80%: 70–130)	Roxburgh et al. (2006) and Luyssaert et al. (2008)	20 (90%: 7–20)	30 (90%: 10–100)
	S,Tr		419 (80%: 377–461)	FAO (2016)	172	1.19 (80%: 1.07–1.31)	Houughton and Nassikas (2018)	60 (80%: 42 to 78)	Pan et al. (2011) and Grace et al. (2014)	15 (90%: 7–20)	20 (90%: 10–100)
Agroforestry (trees in croplands)	T,B	Permanent crop area 2015	100 (80%: 90–110)	Zomer et al. (2016) and Watson et al. (2000);	10 (Zomer et al. 2016)	0.65 (80%: 0.59–0.72)	Nabuurs et al. (2017) and Zomer et al. (2016)	50 (80%: 35 to 65)	Watson et al. (2000)	20 (90%: 7–20)	20 (90%: 10–100)
	S,Tr		300 (66%: 270–330)		30	1.09 (80%: 0.98–1.2)	Ramachdradan Nair et al (2009) and Zomer et al. (2016)	50 (80%: 35–65)	Watson et al. (2000)	15 (90%: 7–20)	20 (90%: 10–100)

example, see Chapter 6 of the Working Group 3 contribution to the Fifth Assessment Report and Chapter 2 of the IPCC Special Report on 1.5 °C. MAGICC has also been used in the preparation of the forthcoming IPCC Sixth Assessment Report to design the GHG concentration scenarios (Meinshausen et al., in preparation).

References

ABS (2017), Australian Bureau of Statistics (2017), Employment in Renewable Energy Activities—Explanatory Notes, for a summary. http://www.abs.gov.au/ausstats/abs@.nsf/Lookup/4631.0Explanatory+Notes12015-16. Accessed September 16, 2018.

Anav, A., et al. (2015), Spatiotemporal patterns of terrestrial gross primary production: A review, Rev. Geophys., 53, 785–818, doi:https://doi.org/10.1002/2015RG000483

Arneth, A., Sitch, S., Pongratz, J., Stocker, B.D., Ciais, P., Poulter, B., Bayer, A.D., Bondeau, A., Calle, L., Chini, L.P., Gasser, T., Fader, M., Friedlingstein, P., Kato, E., Li, W., Lindeskog, M., Nabel, J.E.M.S., Pugh, T.A.M., Robertson, E., Viovy, N., Yue, C., Zaehle, S., 2017. Historical carbon dioxide emissions caused by land-use changes are possibly larger than assumed. Nature Geoscience 10, 79–84. https://doi.org/10.1038/ngeo2882

Asner, G.P., Brodrick, P.G., Philipson, C., Vaughn, N.R., Martin, R.E., Knapp, D.E., Heckler, J., Evans, L.J., Jucker, T., Goossens, B., Stark, D.J., Reynolds, G., Ong, R., Renneboog, N., Kugan, F., Coomes, D.A., 2018. Mapped aboveground carbon stocks to advance forest conservation and recovery in Malaysian Borneo. Biological Conservation 217, 289–310. https://doi.org/10.1016/j.biocon.2017.10.020

Böttcher, H., Herrmann, L. M., Herold, M., Romijn, E., Román-Cuesta, R. M., Avitabile, V., ... & Schepaschenko, D. (2018). Independent Monitoring: Building trust and consensus around GHG data for increased accountability of mitigation in the land use sector.

Breyer (2016), Christian Breyer, Internet of Energy—A 100% renewable electricity system, Neo Carbon Energy, Lappeenranta University of Technology, Finland, 2016, https://www.lut.fi/web/en/news/-/asset_publisher/lGh4SAywhcPu/content/simulation-brings-global-100-renewable-electricity-system-alive-for-the-first-time

Breyer, C, Bogdanov, D (2018), Breyer Ch., Bogdanov D., Aghahosseini A., Gulagi A., Child M., Oyewo A.S., Farfan J., Sadovskaia K., Vainikka P., 2018. Solar Photovoltaics Demand for the Global Energy Transition in the Power Sector, Progress in Photovoltaics: Research and Applications, 26, 505-523, DOI: https://doi.org/10.1002/pip.2950

CIA (2018), Central Intelligence Agency, Library, World Factbook, Online database, viewed in July 2018 https://www.cia.gov/library/publications/the-world-factbook/fields/2195.html

DeCicco, J.M., Schlesinger, W.H., 2018. Reconsidering bioenergy given the urgency of climate protection. Proceedings of the National Academy of Sciences 115, 9642–9645. https://doi.org/10.1073/pnas.1814120115

Dooley, K., Stabinsky, D., Stone, K., Sharma, S., Anderson, T., Gurian-Sherman, D., Riggs, P., 2018. Missing Pathways to 1.5 °C: The role of the land sector in ambitious climate action. Climate, Land, Ambition and Rights Alliance. https://www.climatelandambitionrightsalliance.org/report/

Dunstan C, Fattal, A (2016), Dunstan C., Fattal A., James G., Teske S., 2016, Towards 100% Renewable Energy for Kangaroo Island. Prepared by the Institute for Sustainable Futures, University of Technology Sydney (with assistance from AECOM) for ARENA, Renewables SA and Kangaroo Island Council

Elliston, B, MacGill, Ian (2014), Ben Elliston, Iain MacGill, Mark Diesendorf, Comparing least cost scenarios for 100% renewable electricity with low emission fossil fuel scenarios in the Australian National Electricity, Market, Elsevier, Renewable Energy, Volume 66, June 2014,

Pages 196-204, https://www.sciencedirect.com/science/article/pii/S0960148113006745?via%3Dihub,

EMP-BARCELONA (2002)—Barcelona European Council, 15 and 16 March 2002, Presidency Conclusions. "In the field of Energy the European Council: (…) agrees the target for Member States of a level of electricity interconnections equivalent to at least 10% of their installed production capacity by 2005"; https://cordis.europa.eu/programme/rcn/805_en.html

EU-EG (2017), Towards a sustainable and integrated Europe, Report of the Commission Expert Group on electricity interconnection targets, November 2017, https://ec.europa.eu/info/news/moving-10-15-final-report-commission-expert-group-2030-electricity-interconnection-targets-2017-nov-09_en

FAO, 2016. Global forest resources assessment 2015: how are the world's forests changing? Food and Agriculture Organization of the United Nations

Fischedick, M., R. Schaeffer, A (2011), Fischedick, M., R. Schaeffer, A. Adedoyin, M. Akai, T. Bruckner, L. Clarke, V. Krey, I. Savolainen, S. Teske, D. Ürge-Vorsatz, R. Wright, 2011: Mitigation Potential and Costs. In IPCC Special Report on Renewable Energy, Sources and Climate Change Mitigation [O. Edenhofer, R. Pichs-Madruga, Y. Sokona, K. Seyboth, P. Matschoss, S. Kadner, T. Zwickel, P. Eickemeier, G. Hansen, S. Schlömer, C. von Stechow (eds)], Cambridge University Press, Cambridge, United Kingdom and New York, NY, USA, Chapter 10, http://www.ipcc.ch/pdf/special-reports/srren/Chapter%2010%20Mitigation%20Potential%20and%20Costs.pdf

Flato, G., J. Marotzke, B (2013), Flato, G., J. Marotzke, B. Abiodun, P. Braconnot, S.C. Chou, W. Collins, P. Cox, F. Driouech, S. Emori, V. Eyring, C. Forest, P. Gleckler, E. Guilyardi, C. Jakob, V. Kattsov, C. Reason and M. Rummukainen, 2013: Evaluation of Climate Models. In: Climate Change 2013: The Physical Science Basis. Contribution of Working Group I to the Fifth Assessment Report of the Intergovernmental Panel on Climate Change [Stocker, T.F., D. Qin, G.-K. Plattner, M. Tignor, S.K. Allen, J. Boschung, A. Nauels, Y. Xia, V. Bex and P.M. Midgley (eds.)]. Cambridge University Press, Cambridge, United Kingdom and New York, NY, USA, Chapter 9, http://www.ipcc.ch/pdf/assessment-report/ar5/wg1/WG1AR5_Chapter09_FINAL.pdf

(Global Land Cover 2015); Global Land cover 2000; Joint Research Centre The European Commission's science and knowledge service. 2015. Global Land Cover 2000—Products; Accessed 25 October 2018; ONLINE, http://forobs.jrc.ec.europa.eu/products/glc2000/products.php

(Global Solar Atlas 2016), Global Solar Atlas. 2016; download for varies countries and regions, Accessed 25 October 2018 ONLINE; https://globalsolaratlas.info/downloads

Goodchild, M. F. (2005). GIS and modeling overview. GIS, spatial analysis, and modeling. ESRI Press, Redlands, 1-18. http://www.geog.ucsb.edu/~good/papers/414.pdf

Grace, J., Mitchard, E., Gloor, E., 2014. Perturbations in the carbon budget of the tropics. Global Change Biology 20, 3238–3255. https://doi.org/10.1111/gcb.12600

Gütschow, J., M. L. Jeffery, R. Gieseke, R. Gebel, D. Stevens, M. Krapp and M. Rocha (2016). "The PRIMAP-hist national historical emissions time series." Earth Syst. Sci. Data Discuss. 2016: 1-44.

Hare, B, Roming, N (2016), Hare, B. , Roming, N. , Schaeffer, M. , Schleussner, C., (August 2016), Implications of the 1.5 °C limit in the Paris Agreement for climate policy and decarbonisation, Climate Analytics, Berlin, Germany, Perth, Australia; http://climateanalytics.org/files/1p5_australia_report_ci.pdf

Houghton, R.A., Nassikas, A.A., 2018. Negative emissions from stopping deforestation and forest degradation, globally. Global Change Biology 24, 350–359. https://doi.org/10.1111/gcb.13876

IEA (2016a) World Energy Balances (2016 edition). IEA energy statistics (Beyond 20/20). International Energy Agency, Paris

IEA (2016b) World Energy Outlook 2016. International Energy Agency, Organization for Economic Co-operation and Development, Paris

IEA (2017a) Energy Technology Perspectives. Modelling of the transport sector in the Mobility Model. https://www.iea.org/etp/etpmodel/transport/. Accessed 10 Oct 2018

IEA (2017b) World Energy Outlook 2017. OECD Publishing, Paris/IEA, Paris

IPCC, 2006. Chapter 4: Forest Land, in: 2006 IPCC Guidelines for National Greenhouse Gas Inventories.

IRENA (2017) Renewable Energy Benefits: Leveraging Local Capacity for Onshore Wind, IRENA, Abu Dhabi; http://www.irena.org/-/media/Files/IRENA/Agency/Publication/2017/Jun/IRENA_Leveraging_for_Onshore_Wind_2017.pdf

(Jacobson, M, Choi, C, 2017), Mark Jacobson, Charles Q. Choi, A Road Map to 100 Percent Renewable Energy in 139 Countries by 2050, Stanford Engineering, Stanford University, USA, September 2017, https://cee.stanford.edu/news/road-map-100-percent-renewable-energy-139-countries-2050

Keith, H., Mackey, B.G., Lindenmayer, D.B., 2009. Re-evaluation of forest biomass carbon stocks and lessons from the world's most carbon-dense forests. Proceedings of the National Academy of Sciences 106, 11635–11640. https://doi.org/10.1073/pnas.0901970106

Keith, H., Lindenmayer, D., Macintosh, A., Mackey, B., 2015. Under What Circumstances Do Wood Products from Native Forests Benefit Climate Change Mitigation? PLOS ONE 10, e0139640. https://doi.org/10.1371/journal.pone.0139640

Klaus, T, Vollmer, Clara, (2010), Thomas Klaus, Carla Vollmer, Kathrin Werner, Harry Lehmann, Klaus Müschen, Energy target 2050:100% renewable electricity supply, German Federal Environment Agency, Fraunhofer-Institut für Windenergie und Energiesystemtechnik (IWES), Kassel, Contractor of the research project „Modellierung einer 100-Prozent erneuerbaren Stromerzeugung in 2050",FKZ 363 01 277 Dessau-Roßlau, July 2010, https://www.umwelt-bundesamt.de/sites/default/files/medien/378/publikationen/energieziel_2050_kurz.pdf

Law, B.E., Hudiburg, T.W., Berner, L.T., Kent, J.J., Buotte, P.C., Harmon, M.E., 2018. Land use strategies to mitigate climate change in carbon dense temperate forests. Proceedings of the National Academy of Sciences 115, 3663–3668. https://doi.org/10.1073/pnas.1720064115

Liu, Y.Y., van Dijk, A.I.J.M., de Jeu, R.A.M., Canadell, J.G., McCabe, M.F., Evans, J.P., Wang, G., 2015. Recent reversal in loss of global terrestrial biomass. Nature Climate Change 5, 470–474. https://doi.org/10.1038/nclimate2581

Lutz, J.A., Furniss, T.J., Johnson, D.J., Davies, S.J., Allen, D., Alonso, A., Anderson-Teixeira, K.J., Andrade, A., Baltzer, J., Becker, K.M.L., Blomdahl, E.M., Bourg, N.A., Bunyavejchewin, S., Burslem, D.F.R.P., Cansler, C.A., Cao, K., Cao, M., Cárdenas, D., Chang, L.-W., Chao, K.-J., Chao, W.-C., Chiang, J.-M., Chu, C., Chuyong, G.B., Clay, K., Condit, R., Cordell, S., Dattaraja, H.S., Duque, A., Ewango, C.E.N., Fischer, G.A., Fletcher, C., Freund, J.A., Giardina, C., Germain, S.J., Gilbert, G.S., Hao, Z., Hart, T., Hau, B.C.H., He, F., Hector, A., Howe, R.W., Hsieh, C.-F., Hu, Y.-H., Hubbell, S.P., Inman-Narahari, F.M., Itoh, A., Janík, D., Kassim, A.R., Kenfack, D., Korte, L., Král, K., Larson, A.J., Li, Y., Lin, Y., Liu, S., Lum, S., Ma, K., Makana, J.-R., Malhi, Y., McMahon, S.M., McShea, W.J., Memiaghe, H.R., Mi, X., Morecroft, M., Musili, P.M., Myers, J.A., Novotny, V., de Oliveira, A., Ong, P., Orwig, D.A., Ostertag, R., Parker, G.G., Patankar, R., Phillips, R.P., Reynolds, G., Sack, L., Song, G.-Z.M., Su, S.-H., Sukumar, R., Sun, I.-F., Suresh, H.S., Swanson, M.E., Tan, S., Thomas, D.W., Thompson, J., Uriarte, M., Valencia, R., Vicentini, A., Vrška, T., Wang, X., Weiblen, G.D., Wolf, A., Wu, S.-H., Xu, H., Yamakura, T., Yap, S., Zimmerman, J.K., 2018. Global importance of large-diameter trees. Global Ecology and Biogeography 27, 849–864. https://doi.org/10.1111/geb.12747

Luyssaert, S., Schulze, E.-D., Börner, A., Knohl, A., Hessenmöller, D., Law, B.E., Ciais, P., Grace, J., 2008. Old-growth forests as global carbon sinks. Nature 455, 213–215. https://doi.org/10.1038/nature07276

Mackey, B., 2014. Counting trees, carbon and climate change. The Royal Statistical Society—Significance 19–23.

Mackey, B., Prentice, I.C., Steffen, W., House, J.I., Lindenmayer, D., Keith, H., Berry, S., 2013. Untangling the confusion around land carbon science and climate change mitigation policy. Nature Climate Change 3, 552–557. https://doi.org/10.1038/nclimate1804

Mackey, B., Ware, D., Buckwell, A., Nalau, J., Sahin, O., Flemming, C. M., Smart, J.C., Connollet, R., Hallgren, W., 2018. Options and Implementation for Ecosystem-based Adaptation, Tanna

Island, Vanuatu (No. Report No. ESRAM-3), Griffith Climate Change Response Program. Griffith University, Gold Coast.

Martin, P.A., Newton, A.C., Pfeifer, M., Khoo, M., Bullock, J.M., 2015. Impacts of tropical selective logging on carbon storage and tree species richness: A meta-analysis. Forest Ecology and Management 356, 224–233. https://doi.org/10.1016/j.foreco.2015.07.010

Meinshausen, M., B. Hare, T. M. L. Wigley, D. van Vuuren, M. G. J. den Elzen and R. Swart (2006). "Multi-gas emission pathways to meet climate targets." Climatic Change 75(1): 151–194.

Meinshausen, M., S. C. B. Raper and T. M. L. Wigley (2011). "Emulating coupled atmosphere-ocean and carbon cycle models with a simpler model, MAGICC6: Part I—Model Description and Calibration." Atmospheric Chemistry and Physics 11: 1417-1456.

Müller, R., Pfeifroth, U (2015), Müller, R., Pfeifroth, U., Träger-Chatterjee, C., Trentmann, J., Cremer, R. (2015). Digging the METEOSAT Treasure—3 Decades of Solar Surface Radiation. Remote Sensing 7, 8067–8101. doi: https://doi.org/10.3390/rs70608067

Nabuurs, G.-J., Delacote, P., Ellison, D., Hanewinkel, M., Hetemäki, L., Lindner, M., 2017. By 2050 the Mitigation Effects of EU Forests Could Nearly Double through Climate Smart Forestry. Forests 8, 484. https://doi.org/10.3390/f8120484

Nauels, A., M. Meinshausen, M. Mengel, K. Lorbacher and T. M. L. Wigley (2016). "Synthesizing long-term sea level rise projections—the MAGICC sea level model." Geosci. Model Dev. Discuss. 2016: 1–40.

Pan, Y., Birdsey, R.A., Fang, J., Houghton, R., Kauppi, P.E., Kurz, W.A., Phillips, O.L., Shvidenko, A., Lewis, S.L., Canadell, J.G., Ciais, P., Jackson, R.B., Pacala, S.W., McGuire, A.D., Piao, S., Rautiainen, A., Sitch, S., Hayes, D., 2011. A Large and Persistent Carbon Sink in the World's Forests. Science 333, 988–993. https://doi.org/10.1126/science.1201609

Pfenninger, S, Staffell, I. (2016a), Pfenninger, Stefan and Staffell, Iain (2016). Long-term patterns of European PV output using 30 years of validated hourly reanalysis and satellite data. Energy 114, pp. 1251-1265. doi: https://doi.org/10.1016/j.energy.2016.08.060

Pfenninger, S, Staffell, I. (2016b), Staffell, Iain and Pfenninger, Stefan (2016). Using Bias-Corrected Reanalysis to Simulate Current and Future Wind Power Output. Energy 114, pp. 1224-1239. doi: https://doi.org/10.1016/j.energy.2016.08.068

Pingoud, K., Ekholm, T., Sievänen, R., Huuskonen, S., Hynynen, J., 2018. Trade-offs between forest carbon stocks and harvests in a steady state—A multi-criteria analysis. Journal of Environmental Management 210, 96–103. https://doi.org/10.1016/j.jenvman.2017.12.076

Poorter, L., Bongers, F., Aide, T.M., Almeyda Zambrano, A.M., Balvanera, P., Becknell, J.M., Boukili, V., Brancalion, P.H.S., Broadbent, E.N., Chazdon, R.L., Craven, D., de Almeida-Cortez, J.S., Cabral, G.A.L., de Jong, B.H.J., Denslow, J.S., Dent, D.H., DeWalt, S.J., Dupuy, J.M., Durán, S.M., Espírito-Santo, M.M., Fandino, M.C., César, R.G., Hall, J.S., Hernandez-Stefanoni, J.L., Jakovac, C.C., Junqueira, A.B., Kennard, D., Letcher, S.G., Licona, J.-C., Lohbeck, M., Marín-Spiotta, E., Martínez-Ramos, M., Massoca, P., Meave, J.A., Mesquita, R., Mora, F., Muñoz, R., Muscarella, R., Nunes, Y.R.F., Ochoa-Gaona, S., de Oliveira, A.A., Orihuela-Belmonte, E., Peña-Claros, M., Pérez-García, E.A., Piotto, D., Powers, J.S., Rodríguez-Velázquez, J., Romero-Pérez, I.E., Ruíz, J., Saldarriaga, J.G., Sanchez-Azofeifa, A., Schwartz, N.B., Steininger, M.K., Swenson, N.G., Toledo, M., Uriarte, M., van Breugel, M., van der Wal, H., Veloso, M.D.M., Vester, H.F.M., Vicentini, A., Vieira, I.C.G., Bentos, T.V., Williamson, G.B., Rozendaal, D.M.A., 2016. Biomass resilience of Neotropical secondary forests. Nature 530, 211–214. https://doi.org/10.1038/nature16512

Ramachandran Nair, P.K., Mohan Kumar, B., Nair, V.D., 2009. Agroforestry as a strategy for carbon sequestration. Journal of Plant Nutrition and Soil Science 172, 10–23. https://doi.org/10.1002/jpln.200800030

RE-N DB (2018) Renewables.ninja, onione database for hourly time series for solar and wind data for a specific geographical position, viewed and data down load took place between May and July 2018, https://www.renewables.ninja/

REN21-GSR (2018), 2018; Renewables 2018 Global Status Report, (Paris: REN21 Secretariat), ISBN 978-3-9818911-3-3

Rienecker, M, Suarez MJ, (2011) Rienecker MM, Suarez MJ, Gelaro R, Todling R, et al. (2011). MERRA: NASA's Modern-Era Retrospective Analysis for Research and Applications. Journal of Climate, 24(14): 3624-3648. doi: https://doi.org/10.1175/JCLI-D-11-00015.1

Rogelj, J, den Elzen, M (2016), Joeri Rogelj, Michel den Elzen, Niklas Höhne, Taryn Fransen, Hanna Fekete, Harald Winkler, Roberto Schaeffer, Fu Sha, Keywan Riahi & Malte Meinshausen, (30 June 2016), Paris Agreement climate proposals need a boost to keep warming well below 2 °C, Nature volume 534, pages 631–639 (30 June 2016), https://www.nature.com/articles/nature18307

Roxburgh, S.H., Wood, S.W., Mackey, B.G., Woldendorp, G., Gibbons, P., 2006. Assessing the carbon sequestration potential of managed forests: a case study from temperate Australia: Carbon sequestration potential. Journal of Applied Ecology 43, 1149–1159. https://doi.org/10.1111/j.1365-2664.2006.01221.x

Rutovitz (2015) chapter 7 of: Teske, S, Pregger, T., Naegler, T., Simon, S., Energy [R]evolution—A sustainable

Rutovitz, J., Dominish, E (2015), Rutovitz, J., Dominish, E & Downes, J. (2015) Calculating Global Energy Sector Jobs: 2015 Methodology. Prepared for Greenpeace International by the Institute for Sustainable Futures, University of Technology Sydney.

Rutovitz, J, James, G (2017), Rutovitz, J., James, G., Teske S., Mpofu, S., Usher, J, Morris, T., and Alexander, D. 2017. Storage Requirements for Reliable Electricity in Australia. Report prepared by the Institute for Sustainable Futures for the Australian Council of Learned Academies.

Sarah (2018) – Online database of "renewable.ninja," https://dx.doi.org/10.5676/EUM_SAF_CM/SARAH/V001

Schlenzig C (1998) Energy planning and environmental management with the information and decision support system MESAP. International Journal of Global Energy Issues, 12(1–6):81–91.

Seven2one (2012) Mesap/PlaNet software framework: Seven2one Modelling, Mesap4, Release 4.14.1.9, Seven2one Informationssysteme GmbH, Karlsruhe, Germany

Simon S, Naegler T, Gils H (2018) Transformation towards a Renewable Energy System in Brazil and Mexico—Technological and Structural Options for Latin America. Energies 11 (4):907

ST 7 (2018), Statistic Times viewed July 2018, http://statisticstimes.com/economy/countries-by-gdp-sector-composition.php

Teske, S (2015), Thesis, Bridging the Gap between Energy- and Grid Models, Developing an integrated infrastructural planning model for 100% renewable energy systems in order to optimize the interaction of flexible power generation, smart grids and storage technologies, chapter 2, University Flensburg, Germany

Teske, S, Brown, T, (2012), Teske, S, Dr. Tom Brown, Dr. Eckehard Tröster, Peter-Philipp Schierhorn, Dr. Thomas

Teske, S, Dominish, E (2016), Teske, S., Dominish, E., Ison, N. and Maras, K. (2016) 100% Renewable Energy for Australia—Decarbonising Australia's Energy Sector within one Generation; Report prepared by ISF for GetUp! and Solar Citizens, March 2016, https://www.uts.edu.au/sites/default/files/article/downloads/ISF_100%25_Australian_Renewable_Energy_Report.pdf

Teske, S, Morris, T (2017), Teske, S., Morris, T., Nagrath, Kriti (2017) 100% Renewable Energy for Tanzania—Access to renewable and affordable energy for all within one generation. Report prepared by ISF for Bread for the World, October 2017.

Teske, S, Pregger, T (2015), Teske, S, Pregger, T., Naegler, T., Simon, S., Energy [R]evolution—A sustainable World Energy Outlook 2015, Greenpeace International with the German Aerospace Centre (DLR), Institute of Engineering Thermodynamics, System Analysis and Technology Assessment, Stuttgart, Germany. https://www.scribd.com/document/333565532/Energy-Revolution-2015-Full

UN PD DB (2018) United Nations, Population Division, online database, viewed June 2018—https://population.un.org/Household/index.html#/countries

UNFCCC (2015), The Paris Agreement builds upon the Convention and for the first time brings all nations into a common cause to undertake ambitious efforts to combat climate change and adapt to its effects, with enhanced support to assist developing countries to do so. As such,

it charts a new course in the global climate effort. https://unfccc.int/process-and-meetings/the-paris-agreement/the-paris-agreement

(Vaisala 2017) Free Wind and Solar Resource Maps; Accessed 25 October 2018; ONLINE; https://www.vaisala.com/en/lp/free-wind-and-solar-resource-maps.

Watson, B., Noble, L., Bolin, B., et. al., 2000. Summary for policymakers: land use, land-use change, and forestry: a special report of the Intergovernmental Panel on Climate Change. Intergovernmental Panel on Climate Change.

WEC (2018) World Energy Council—Energy Efficiency Indicators, Online database, viewed June 2018), https://wec-indicators.enerdata.net/specific-electricity-use.html

Wheeler, C., Mitchard, E., Koch, A., Lewis, S.L., in press. The mitigation potential of large-scale tropical forest restoration: assessing the promise of the Bonn Challenge. in review.

WRI (2018), World Resources Institute, A Global Database of Power Plants, April 2018, viewed in July 2018, http://www.wri.org/publication/global-power-plant-database

Ziegler, A.D., Phelps, J., Yuen, J.Q., Webb, E.L., Lawrence, D., Fox, J.M., Bruun, T.B., Leisz, S.J., Ryan, C.M., Dressler, W., Mertz, O., Pascual, U., Padoch, C., Koh, L.P., 2012. Carbon outcomes of major land-cover transitions in SE Asia: great uncertainties and REDD+ policy implications. Global Change Biology 18, 3087–3099. https://doi.org/10.1111/j.1365-2486.2012.02747.x

Zimmerman, B., Kormos, C., 2012. Prospects for Sustainable Logging in Tropical Forests. BioScience 62, 479–487. https://doi.org/10.1525/bio.2012.62.5.9

Zomer, R.J., Neufeldt, H., Xu, J., Ahrends, A., Bossio, D., Trabucco, A., van Noordwijk, M., Wang, M., 2016. Global Tree Cover and Biomass Carbon on Agricultural Land: The contribution of agroforestry to global and national carbon budgets. Scientific Reports 6. https://doi.org/10.1038/srep29987